LAWRENCE
LIVERMORE
NATIONAL
LABORATORY

LLNL-JRNL-462784

A Geochemical and Sedimentary Record of High Southern Latitude Holocene Climate Evolution from Lago Fagnano, Tierra del Fuego

C. M. Moy, R. B. Dunbar, T. P. Guilderson, N. Waldmann, D. A. Mucciarone, C. Recasens, J. A. Austin, F. S. Anselmetti

November 19, 2010

Earth and Planetary Sciences Letters

Disclaimer

A Geochemical and Sedimentary Record of High Southern Latitude Holocene Climate Evolution from Lago Fagnano, Tierra del Fuego

Christopher M. Moy[1*], Robert B. Dunbar[2], Thomas P. Guilderson[3], Nicolas Waldmann[4], David A. Mucciarone[2], Cristina Recasens[5], Daniel Ariztegui[5], James A. Austin, Jr.[6] and Flavio S. Anselmetti[7]

[1]Dept. of Geological and Environmental Sciences, 450 Serra Mall, Braun Hall (Bldg. 320), Stanford University, Stanford, CA 94305-2115 USA; moyc@stanford.edu

[2]Dept. of Environmental Earth System Science, 450 Serra Mall, Braun Hall (Bldg. 320), Stanford University, Stanford, CA 94305-2115 USA; dunbar@stanford.edu; dam@stanford.edu

[3]Center for Accelerator Mass Spectrometry, Lawrence Livermore National Laboratory, L-397, 7000 East Ave., Livermore, CA 94550 USA; tguilderson@llnl.gov

[4]Dept. of Earth Science, University of Bergen, Allegt 41, 5007 Bergen, Norway; Nicolas.Waldmann@geo.uib.no

[5]Dept. of Geology and Paleontology, University of Geneva, 13, Rue des Maraîchers, CH-1205 Genève, Switzerland; Cristina.Recasens@unige.ch; daniel.ariztegui@unige.ch

[6]Institute for Geophysics, John A. and Katherine G. Jackson School of Geosciences, The University of Texas at Austin, Bldg. 196 (ROC); 10100 Burnet Road (R2200); Austin TX 78758-4445; jamie@ig.utexas.edu

[7]EAWAG, Swiss Federal Institute of Aquatic Science and Technology, Department of Surface Waters, Überlandstrasse 133, CH-8600 Dübendorf, Switzerland; flavio.anselmetti@eawag.ch

*Present affiliation: Geology Department, University of Otago, P.O. Box 56, Dunedin 9054, New Zealand; chris.moy@otago.ac.nz;

**Current contact information (On research leave until March 2011):

U.S. Geological Survey, Woods Hole Coastal and Marine Science Center, 384 Woods Hole Road, Woods Hole, MA 02543 phone: +1.650.380.0395; fax: +1.508.457.2310; e-mail: moyc@stanford.edu

Keywords: Southern Hemisphere Westerly Winds, Holocene Paleoclimate, Radiocarbon, Stable Isotopes, Tierra del Fuego

Abstract

Situated at the southern margin of the hemispheric westerly wind belt and immediately north of the Antarctic Polar Frontal zone, Tierra del Fuego is well-positioned to monitor coupled changes in the ocean-atmosphere system of the high southern latitudes. Here we describe a Holocene paleoclimate record from sediment cores obtained from Lago Fagnano, a large lake in southern Tierra del Fuego at 55°S, to investigate past changes in climate related to these two important features of the global climate system. We use an AMS radiocarbon chronology for the last 8,000 years based on pollen concentrates, thereby avoiding contamination from bedrock-derived lignite. Our chronology is consistent with a tephrochronologic age date for deposits from the middle Holocene Volcán Hudson eruption. Combining bulk organic isotopic ($\delta^{13}C$ & $\delta^{15}N$) and elemental (C & N) parameters with physical sediment properties allow us to better understand sediment provenance and transport mechanisms and to interpret Holocene climate and tectonic change during the last 8,000 years. Co-variability and long-term trends in C/N ratio, carbon accumulation rate, and magnetic susceptibility reflect an overall Holocene increase in the delivery of terrestrial organic and lithogenic material to the deep eastern basin. We attribute this variability to westerly wind-derived precipitation. Increased wind strength and precipitation in the late Holocene drives the *Nothofagus* forest eastward and enhances run-off and terrigenous inputs to the lake. Superimposed on the long-term trend are a series of abrupt 9 negative departures in C/N ratio, which constrain the presence of seismically-driven mass flow events in the record. We identify an increase in bulk $\delta^{13}C$ between 7,000 and 5,000 cal yr BP that we attribute to enhanced aquatic productivity driven by warmer summer temperatures. The Lago Fagnano $\delta^{13}C$ record shows similarities with Holocene records of sea surface temperature from the mid-latitude Chilean continental shelf and Antarctic air temperatures from the Taylor Dome ice core record in East Antarctica. Mid-Holocene warming occurred simultaneously across the Antarctic Frontal Zone, and in particular, in locations currently influenced by the Antarctic Circumpolar Current.

1. Introduction

Southernmost South America is well-located to address questions related to Holocene climate change in the mid- to high-latitudes of the Southern Hemisphere. The island of Tierra del Fuego is located at the southern margin of the modern westerly winds and 5° north of the Antarctic Frontal Zone (AFZ). The strength of the westerlies at this latitude drives the Antarctic Circumpolar Current (ACC), Ekman divergence, and ultimately, the upwelling of CO_2-rich deepwater that can influence global CO_2 flux variability over interannual (Le Quéré et al., 2007; Lovenduski et al., 2007) to glacial – interglacial timescales (Toggweiler et al., 2006). In addition to its impact on the global and hemispheric meridional overturning circulation, the strength of the overlying zonal atmospheric flow plays a significant role in regional precipitation regimes (Garreaud, 2007; Garreaud et al., 2009; Moy et al., 2009) and has been shown to be an important driver of Holocene climate change in Patagonia at centennial- to millennial-timescales (Moreno et al., 2009a; Moy et al., 2008). Farther to the south, the AFZ represents a greater than 6°C decrease in sea surface temperatures (SST) that marks the boundary between the cold polar high latitudes and the temperate mid-latitudes of the Southern Hemisphere (Belkin and Gordon, 1996). Past northward migrations in the Polar Frontal Zone (PFZ) have been invoked to explain colder temperatures and expansion of ice from the Cordillera Darwin and Southern Patagonian ice sheets during the Last Glacial Maximum and the Late Glacial (Kaplan et al., 2008; Moreno et al., 2009b). Paleoclimate records from Tierra del Fuego provide a much-needed terrestrial perspective on past changes in the ocean-atmosphere system in the southern high latitudes.

Previous paleoclimate records used to reconstruct Holocene and Late Glacial climate variability in Tierra del Fuego have used: (1) stratigraphy and radiocarbon ages on glacial deposits (Clapperton et al., 1995; Kaplan et al., 2008; Kaplan et al., 2007; Kuylenstierna et al., 1996; McCulloch and Bentley, 1998; McCulloch et al., 2005; Mercer, 1982; Strelin et al., 2001), (2) paleoclimate and paleoecological records recovered from lakes and bogs (Heusser et al., 2000; Heusser and Rabassa, 1987; Heusser and Rabassa, 1995; Markgraf, 1993; Mauquoy et al., 2004; Pendall et al., 2001; Waldmann et al., 2010a), (3) tree-ring

94 temperature reconstructions (Aravena et al., 2002; Boninsegna et al., 1990) and (4) aeolian dust flux
95 reconstructions from peat deposits (Sapkota et al., 2007). Continuous well-dated Holocene lacustrine
96 sediment records are as yet notably missing from Tierra del Fuego, yet they can fully exploit the location
97 and its link to modern climate and are not subject to the uncertainties of the marine reservoir age
98 correction that all Southern Ocean records must surmount (Hodell et al., 2001; Nielsen et al., 2004; van
99 Beek et al., 2002). Sediment records from larger lakes are particularly relevant because they integrate
100 climate signals over a larger region, are less susceptible than smaller lakes to non-climatic local effects,
101 and can offer homogenous depositional environments that aid proxy development. A prerequisite for any
102 paleoclimate interpretation from lacustrine sediment cores is knowledge of (1) overall basin architecture
103 and stratigraphy, (2) sediment provenance and delivery mechanisms/pathways, and (3) sediment
104 lithologies. Furthermore, the establishment of a reliable radiocarbon chronology requires knowledge of
105 the geologic context of organic material to be dated (Björck and Wohlfarth, 2001; Olsson, 1991).
106 In 2005 and 2006, we undertook a high-resolution seismic survey followed by sediment coring
107 from presumed high-accumulation rate sedimentary sequences within Lago Fagnano, a long (> 100 km),
108 linear, E-W orientated oligotrophic lake with maximum water depths exceeding 200 meters (Figure 1).
109 The lake is situated along a major plate boundary and occupies a deep continental pull-apart basin
110 associated with the Magellan-Fagnano Transform system (Lodolo et al., 2003) that has been sculpted and
111 over-deepened by successive Quaternary glaciations. Lago Fagnano is an "open-system" lake with a
112 single spillway to the Pacific Ocean via the Río Azopardo and is fed by numerous small streams and
113 rivers. Descriptions of the principal sub-basins, seismic stratigraphy, and general sediment core
114 stratigraphy were presented by Waldmann et al., (2008), Waldmann et al., (2010a), and Waldmann et al.
115 (2010b).

116 Waldmann et al. (2010a) describe the physical and bulk chemical properties of sediment cores
117 collected from Lago Fagnano sub-basins and use these parameters, in part, to infer westerly wind
118 variability during the Holocene. The authors focus on downcore variations in solid phase Fe abundance

obtained from a profiling XRF scanner to infer changes in the influx of detrital magnetic minerals, which they argue is indirectly controlled by regional precipitation (Waldmann et al., 2010a). Higher precipitation causes greater influx of magnetic minerals to the deep isolated sub-basins within the lake. A prominent decline in Fe through the Holocene towards modern argues for a reduction in westerly derived precipitation, an inference that is opposite from existing records in the region (Huber et al., 2004, Markgraf and Huber, 2010, Moreno et al., 2009). Moreover, magnetic susceptibility levels in all cores collected in the eastern basin increase through the Holocene, signaling an overall increase in the abundance of ferromagnetic minerals that might be associated with enhanced runoff (increased westerlies). Fe abundance, however, is difficult to interpret in lacustrine systems as its presence in sediments can be controlled by diagenetic alteration and is further complicated by dilution effects (Löwemark et al., 2010), bulk density, mineralogy and grain size changes (Croudace et al., 2006). In order to better understand past variations in the precipitation regime, and by extension, the westerly wind field from Lago Fagnano sediments, we have developed a paleoclimate record using proxies derived from our understanding of drainage basin processes.

In this paper, we present a Holocene record of climatically- and tectonically-induced sedimentation from Lago Fagnano with foci on: 1) understanding changes in sediment provenance and delivery mechanisms to the deep eastern basin, 2) establishing a testable/verifiable radiocarbon chronology that can be used to constrain the timing of past climate/tectonic events; and 3) contributing to our understanding of climate variability in high southern latitudes. We examine piston core and surface sediment samples obtained from the >180-meter deep eastern sub-basin and apply a multi-proxy approach combining bulk organic geochemistry (C and N), physical sediment properties, and wt. % biogenic silica to characterize changes in aquatic productivity, drainage basin erosion, and tectonically-induced mass-wasting events, and ultimately, better understand past variations in climate in this important geographical locale. Bulk organic isotopes ($\delta^{13}C$ and $\delta^{15}N$) and concentrations are used to infer past changes in aquatic productivity and sediment provenance as has been accomplished in other large lake systems in South

America including Lago Titicaca (Rowe et al., 2003), Lago Puyehue (Bertrand et al., 2009), Laguna Potrok Aike (Haberzettl et al., 2007), and Laguna Azul (Mayr et al., 2005). We also combine our bulk organic geochemistry measurements with a pollen AMS radiocarbon chronology to characterize Holocene changes in climate. The paleoclimate interpretations, and to a greater extent, the radiocarbon chronology, presented in this paper supersedes previous work from the lake and provides a more comprehensive and up-to-date understanding of Holocene climate change in Tierra del Fuego.

2. Study Area

Lago Fagnano (Figure 1) extends for ~100 km E/W along the southern margin of Tierra del Fuego parallel to but north of the Beagle Channel (54°S, 68°W, 26 meters above sea level). The lake occupies a deep basin within the left-lateral Magellan-Fagnano Transform fault system, an active tectonic boundary separating the Scotia and South American plates with estimated horizontal slip rates of 6.6 $\pm$ 1.3 mm/year (Lodolo et al., 2003; Smalley et al., 2003). The fault system extends across the island of Tierra del Fuego through Lago Fagnano and bends across the Strait of Magellan along its northwest arm (Lodolo et al., 2003). Traces of the transform fault on land are manifest as sag ponds, fault scarps, linear truncation of drainage patterns, and deformation and extension of late Quaternary glacial sediments to the east of the lake (Menichetti et al., 2008). Today, relatively low levels of seismicity (Richter magnitude < 3.5) are recorded along the fault system, but large earthquakes have been recorded in the past, most notably the destructive 1949 earthquake (7.5 Richter magnitude), which triggered landslides within the watershed and displaced the Río Turbio to the east of the lake (Menichetti et al., 2008). The lake is bounded by a set of low elevation (<1500 meters) mountain ranges – the Sierra de Beauvoir and Sierra Las Pinturas to the north and the Sierra Alvear to the south – that taper eastwards in elevation and represent an eastern extension of the higher and still glaciated Cordillera Darwin (Figure 1). Small alpine glaciers occupy cirques at elevations greater than 1,000 meters in the Cordillera Darwin and a few of these small glaciers discharge minor amounts of meltwater to the westernmost part of the lake (Figure 1b). The NE section of the lake exposes folded lower Paleogene Río Claro Group marine foreland basin deposits consisting of conglomerates, sandstones, siltstones and coal-bearing mudstones, while outcrops

to the south and west of the lake expose Cretaceous marine slope metasediments (Beauvoir Formation) and upper Jurassic metamorphosed volcanic and sedimentary sequences (Lemaire Formation) (Olivero and Malumián, 2008). Poorly consolidated late Quaternary glacial diamict, glaciolacustrine, and glaciofluvial deposits are common along the northern and southern shores of the lake (Bujalesky et al., 1997).

Lago Fagnano can be divided into two sedimentary basins referred to as the western and eastern sub-basins (Figure 2a). Waldmann et al. (2008, 2010a, 2010b) describe the sequence stratigraphy of the sediments filling these two sub-basins using seismic data acquired from high-resolution single channel (3.5 kHz "pinger") and multichannel (1 in^3 airgun) geophysical methods. By combining these two techniques, the authors characterize the Lago Fagnano basin architecture as consisting of a complex bedrock morphology overlain by >100 m of glacial and lacustrine infill. The sedimentary sequence in the eastern basin has been subdivided into three units (from bottom to top): (1) Unit EA, a thick, transparent, and chaotic basal unit interpreted as glacially-derived sediments, (2) Unit EB, comprising transparent subunits separated by almost equally spaced continuous medium- to high-amplitude reflections representing sequences of glacio-lacustrine sediments, overlain by (3) Unit EC, consisting of intercalated thinly spaced, high-amplitude internal reflections with low-amplitude to transparent intervals reflecting pelagic/lacustrine conditions interbedded with downslope mass-flow events (Waldmann et al., 2010a). We targeted the deeper eastern sub-basin for development of a paleoclimate record (Figure 2b) because it contains the thickest apparently undisturbed sequence of Unit EC in Lago Fagnano (Figure 2c). Sediment cores PC-18 (presented here) and PC-16 (Waldmann et al., 2010a) collected in 185 m water depth penetrate Unit EC and consist of pelagic lacustrine silts and clays intercalated with thin (<15 cm thick) downslope mass-flow (turbidite) deposits.

The modern climate of Lago Fagnano can be characterized as semi-arid and cold with mean annual precipitation and temperature of 550 mm and 6°C, respectively. In February 2004, we established a tripod-mounted, automated weather station at the Argentine Prefectura station on the southern shore of

Lago Fagnano (Figure 1b). With the exception of two minor service interruptions (< 2 months), the station continuously recorded hourly temperature, relative humidity, barometric pressure, wind speed and direction, and precipitation measurements. From this data set, we have compiled monthly climatologies of wind direction (Supplemental Figure 1a), temperature, wind speed and precipitation (Supplemental Figure 1b). The average annual air temperature at the lake is 5.8°C, with summer and winter temperatures averaging 9°C and 1°C, respectively. Lakeshore wind velocities are highest during the austral summer (January – March) and lowest during the winter months (June – July), when the core of the mid-latitude jet is situated farther to the north. Precipitation generally follows the annual cycle in wind speed, with maximum rainfall recorded during the summer months. Precipitation amounts measured at the Lago Fagnano station are generally less than in Ushuaia (the closest permanent weather station) except in November, likely reflecting a small rain shadow effect from the surrounding Sierra de Alvear. A wind rose diagram calculated from the station data shows a bimodal distribution in relative wind direction frequency: recorded winds are mostly out of the southwest, but stronger northwesterly winds are also common (Supplemental Figure 1a).

3. Materials and Methods

Sediment cores were collected during field campaigns in 2005 and 2006 using a Kullenberg-type piston coring system on the 11-m long vessel *R/V Neecho*. Coring locations in the eastern sub-basin were selected based on the seismic stratigraphy and are mostly free of mass flow and large-scale (eroding) turbidite deposits. The piston core PC-18 and gravity core LF-01 described here were collected in 185 meters of water and have total lengths of 527 and 215 cm, respectively. Although PC-18 appears to contain the sediment-water interface, additional short gravity cores (<2.5 m) were recovered and a series of sediment "grab" samples were collected with a modified Ekman dredge from a variety of depths and distances from fluvial inputs to the lake (Figure 2b). In addition to sediment samples, *Nothofagus pumilio* and *N. antarctica* leaves, litter, and underlying surficial soil horizons were sampled from locations within the Fagnano watershed in order to constrain the isotopic signatures of organic matter entering the lake.

Physical sediment properties, including bulk density, magnetic susceptibility, and P-wave velocity, were measured on the PC-18 and LF01 sediment cores at 1-cm resolution using a Geotek Multi-Sensor Core Logger at ETH (Zurich, Switzerland) and at the USGS Coastal and Marine Geology facility (Menlo Park, CA), respectively. Sediment cores were split, described and immediately photographed in order to preserve fine mm-scale laminae that quickly fade upon exposure to the atmosphere.

We obtained continuous 3 ml samples at 1 cm resolution for bulk organic C and N isotope and concentration analysis (C and N). Samples were oven dried at 40°C, weighed into tin capsules, and analyzed on a Carlo Erba NA1500 Series 2 elemental analyzer coupled to a Finnigan Delta Plus isotope ratio mass spectrometer via a Finnigan Conflo II open split interface at the Stanford University Stable Isotope Biogeochemistry Laboratory (SIBL). Results are presented in standard delta notation with $\delta^{13}C$ reported relative to the VPDB carbonate standard and $\delta^{15}N$ relative to air. The average standard deviation of replicate samples was 0.06‰ for $\delta^{13}C$, 0.32‰ for $\delta^{15}N$, and 0.01 % for C and N concentrations (n=23). Biogenic silica (wt. % BSi) was measured at 3 cm resolution by spectrophotometry after NaOH leaching and extraction after 2, 3 and 4 hours using a method modified from Mortlock and Froelich (1989) and DeMaster (1981). The average standard deviation of replicate samples using this method was 0.11% (n=7).

A total of 12 horizons were selected for radiocarbon dating in the LF01 and PC-18 sediment cores (Table 1). AMS radiocarbon ages were obtained on a variety of materials, including bulk organic sediment, terrestrial macrofossils and pollen concentrates. Because coal (lignite) has been identified as a contaminant in paleoclimate studies across Tierra del Fuego (Heusser, 1999; McCulloch et al., 2005) and is present in sedimentary rocks within the Lago Fagnano drainage basin (Olivero and Malumián, 2008), we focus our radiocarbon dating scheme on pollen concentrates. AMS dating of pollen extracts is a reliable method for obtaining accurate radiocarbon ages and surmounting contamination difficulties introduced by older or radiocarbon-"dead" material (Brown et al., 1989; Mensing and Southon, 1999; Piotrowska et al., 2004; Vandergoes and Prior, 2003). Moreover, pollen is considered a reliable material

to date in lacustrine settings because trees and pollen are typically in isotopic equilibrium with the atmospheric radiocarbon pool, rather than the lacustrine dissolved inorganic carbon (DIC) pool (as is the case for lacustrine macrophytes), which can have contributions of old DIC from groundwater/bedrock sources (e.g. Chondrogianni et al., 2004). We found that a method developed by Vandergoes and Prior (2003), which combines a modified method of pollen extraction from lake sediments (e.g., Faegri and Iverson (1989), but excluding the use of C-containing acids/solvents) with stepwise liquid density separation, works best for our samples. A total of 15 grams of wet sediment obtained from 1.0 to 1.5 cm thick sections of core was digested using 10% HCL, 50% HF, 10% HNO_3, and 10% KOH. The remaining material was sieved at 125μm and then passed through a series of heavy liquid density separations using sodium metatungstate. After an initial pass using a solution with a specific gravity of 2.1 to separate dense inorganic material from pollen, successive separation cycles were carried out, starting with specific gravity of 1.8 and decreasing to 1.1 at an interval of 0.1. Individual specific density separates were obtained from 1.6 to 1.1 and those with the highest pollen yield that were free of black particulates (presumably dead C contaminants), as identified after inspection under a binocular microscope, were selected for dating. The selected pollen concentrates were acidified with 1N HCl to remove any absorbed atmospheric CO_2 before multiple DI rinses, combustion, conversion to graphite, and analysis at the Center for Accelerator Mass Spectrometry (CAMS) at Lawrence Livermore National Lab. Radiocarbon dates were converted to calendar years BP (cal yr BP) using Calib 6.0 (Stuiver and Reimer, 1993) using the Southern Hemisphere calibration curve (McCormac et al., 2004). We established an age model for the PC-18 sediment core by applying a linear regression through the median probability ages derived from Calib 6.0 (Table 1).

4. Results

4.1 – Sediment core stratigraphy

Piston core PC-18 and gravity core LF01 recovered the uppermost section of Unit EC in the deep eastern sub-basin (Figure 2). The uppermost 230 cm in PC-18 and the entire LF01 core consist of brown silty clay, with dark 0.5 – 2 mm laminae that oxidize and fade rapidly after exposure. The laminated

interval is truncated by a series of nine 1-15 cm thick light-colored sedimentary units that consist of graded and fining upwards silt and sand. A complex change in sedimentology occurs at mid-depth (~230 cm) in the PC-18 sediment core. A 7 cm thick coarse graded sand unit unconformably overlies a 10 cm thick laminated interval, a 3 cm thick tephra, and ~300 cm of deformed and mottled inorganic silts that extend to the base of the PC-18 core (Figure 3). The 7 cm thick sand unit with a scoured erosive base overlies the mobilized and deformed sediments (including the reworked tephra) and effectively divides the PC-18 core into a lower chaotic (disturbed) section, representing a mass wasting deposit, and an upper relatively undisturbed and laminated section (Figure 3). The intermediate graded sand likely represents a turbidite that typically follows large-scale downslope sediment mobilization and overlies the mass flow deposit (Schnellmann et al., 2005). We focus our geochemical measurements on the upper undisturbed section (0-230 cm) of the PC-18 core.

4.2 – Bulk Density

Bulk sediment density in the upper 230 cm of the PC-18 piston core averages 1.5 g/cc and exhibits a small (<0.2 g/cc) negative trend towards the top of the core. Superimposed on the trend are nine abrupt positive increases in bulk density that correspond to the light-colored and graded silty-sandy sedimentary units described above (Supplemental Figure 2). Positive excursions in the PC-18 density profile are also correlative with density peaks in the LF01 and PC-16 sediment cores (Waldmann et al., 2010a) obtained within 2km of the PC-18 core in the eastern basin (Figure 2 and Supplemental Figure 2) reflecting the basinwide and complete nature of the recovered lithologic succession.

4.3 – Bulk organic geochemistry and biogenic silica

Bulk organic geochemistry and wt. % BSi results are presented in Figure 4. Carbon and nitrogen concentrations increase monotonically from the base of the undisturbed section at 230 cm to the top of the core. C/N generally follows this positive long-term trend in elemental concentration, but displays a series of 9 abrupt departures and a single large excursion at the top of the core (Figure 4). There is a systematic pattern associated with these 9 negative departures in C/N ratio. C/N ratio abruptly rises, quickly falls,

and then re-attains its original values. The bulk organic $\delta^{13}C$ profile exhibits a total range of < 2‰ throughout the PC-18 sediment core (Figure 4). The base of the core has relatively low values (mean of -25.8‰) overlain by a section that averages -25.2‰ at 150 cm. Bulk organic $\delta^{13}C$ gradually decreases from 150 cm to the lowest values in the record at the core top (-26.6‰). Abrupt 0.25 – 0.5‰ decreases in $\delta^{13}C$ correspond with the initial rise and rapid decline in C/N values in the core. Sedimentary $\delta^{15}N$ displays 2-3‰ variability at the base of the core followed by low frequency variations with maximum values at 130 and 25 cm with intervening low values at 175 and 75 cm. Wt.% BSi averages 3.5% throughout PC-18; abrupt 2% declines are correlative with reductions in C/N and carbon and nitrogen concentrations.

4.4 – Radiocarbon chronology

We present two age-depth models for the PC-18 core in Figure 5 and summarize the results in Table 1. The bulk organic C, pollen concentrate, and terrestrial macrofossil radiocarbon dates obtained on the LF01 core were composited with dates from PC-18 using the bulk density profiles (Supplemental Figure 2) for core-to-core correlation. Bulk sedimentary radiocarbon dates obtained from the sediment-water interface and 4 lower horizons exhibit significantly older ages (>5000 years) than corresponding pollen concentrate ages taken from similar depths (Figure 5). With the exception of the 6,500 cal yr sediment-water interface date, the remaining bulk dates are in stratigraphic order and exhibit a 5000 to 7000 cal yr offset from corresponding pollen dates. In two out of three cases, the terrestrial macrofossil dates are older than dates obtained on nearby pollen concentrates – the exception is the macrofossil date at 153 cm (see below). Reproducibility of pollen dates precipitated from specific gravities of 1.3 and 1.6 at 65 cm is <300 cal years BP and provides a minimum error estimate for our chronology.

5. Discussion

5.1 Radiocarbon contamination and the construction of a reliable age model

Three factors complicate the construction of a reliable radiocarbon chronology in Lago Fagnano sediments: (1) low concentrations of suitable/relevant organic material in cored sediments, (2) potential contamination by old or “dead” carbon sources within the watershed, and (3) remobilization and

deposition of older lacustrine or glacial sediments. Obtaining a continuous sedimentary sequence with minimal turbidite disturbance in Lago Fagnano requires core recovery from the center of the deep eastern sub-basin, which by virtue of its distance from shore, contains very few terrestrial macrofossils. In fact, the limited terrestrial macrofossils (principally wood fragments) that are present in the PC-18, LF01, and PC-16 sediment cores are associated with turbidites and presumably were transported downslope from littoral or other areas of the lake during mass flow events (Waldmann et al., 2010b). In addition to the questionable context of terrestrial macrofossils, the Fagnano watershed contains multiple old or "dead" carbon sources that can contaminate bulk organic material. Principal contamination sources include the poorly consolidated late Pleistocene glacial material exposed along the shoreline and the coal-bearing Paleogene mudstones that outcrop immediately to the north of the deep eastern basin. Finally, reworking associated with seismically-driven sediment gravity flow events may involve the erosion of older lacustrine material from shallower areas of the lake and redeposition within the center of the deep basin. Despite these difficulties, by combining radiocarbon dates on concentrated pollen extracts with our knowledge of sediment provenance from bulk organic chemistry and physical sediment properties, we can surmount these obstacles and construct a reliable sediment core chronology.

Our first attempt at establishing a radiocarbon chronology for the eastern sub-basin has consisted of analyzing bulk organic sediment from five horizons including the sediment-water interface from the LF01 core (Figure 5 and Table 1). Radiocarbon dates obtained on the bulk acid- and base-insoluble residue have revealed a core-top age 6150 ^{14}C yr BP, an age reversal between the core top and the date below at 45 cm, followed by successively older dates down to 157 cm. Based on the high-resolution seismic data and knowledge of the timing of sediment deposition with respect to know glacial events in the region (Kaplan et al., 2008; McCulloch et al., 2005), the ages obtained from bulk sedimentary dates are too old and must be non-representative of the actual timing of sediment deposition. Radiocarbon dates obtained on the pollen concentrates, however, produce a radiocarbon stratigraphy with no reversals, a linear sedimentation rate, and a basal date of ~6,000 cal yr BP (Figure 5). Although we elected not to date the sediment-water interface, as it immediately overlies an interpreted turbidite deposit and therefore

might be altered (see below), there are four paired pollen concentrate and bulk dates that exhibit offsets between 5,000 and 7,500 cal yr BP. Two dates obtained from the same depth horizon, but precipitated from the heavy liquid at 1.3 and 1.6 g/cm^3, are 10 years outside the 2 σ radiocarbon calibration range (within 300 ^{14}C years). This age discrepancy may reflect heterogeneity in the 1.5 cm thick (15 g wet sediment) sample. The terrestrial macrofossil radiocarbon dates are generally older than proximal pollen dates, with the exception of radiocarbon dates obtained at 153 cm, which appear to be derived from a turbidite interval and are excluded from our age model (Figure 5). The older pollen concentrate date (relative to the macrofossil radiocarbon age) at 153 cm may signal minor reworking of pollen and/or heterogeneity within the turbidite deposit.

We developed an age model for the PC-18 core by first removing the nine turbidite units using the density and organic geochemistry stratigraphy (see below) and placing a linear regression through the median probability calibrated pollen dates (Figure 5b). To some extent, we can test the accuracy of our age models by comparing the published age of the Holocene Volcán Hudson (H1) tephra with the constructed age model. The H1 tephra is present in both the PC-18 and PC-16 sediment cores and has been geochemically identified by Waldmann et al. (2010a). The mean pooled age obtained from the 10 most representative ages for this explosive eruption (see Figure 1 for location in central Patagonia) is 6850 $\pm$ 160 ^{14}C, which yields a 2σ calibrated age range of 7420 – 7960 cal yr BP and a median calibrated age of 7660 (Stern, 2008). Although it is tempting to use the age of the tephra to rigorously test our age model, the location of the ash layer within the turbidite precludes an exact age/depth assignment for the PC-18 core (see Figure 3). In this case, the mean pooled age for the H1 essentially represents a maximum limiting age and our pollen concentrate chronology is in agreement with this (i.e. it is older than our pollen ages; see Figure 5). Overall, given the 300 year reproducibility of pollen concentrate ages, we take a conservative approach and estimate that the chronology presented here is accurate to 500 years during the Holocene.

372 Dead carbon derived from coal deposits in the lower Paleogene sedimentary exposures directly
373 north of the eastern sub-basin (Figure 1) is the likely cause of the radiocarbon contamination in Lago
374 Fagnano sediments. In Puerto del Hambre (230 km NW) Heusser (1999) reported contamination by
375 "infinitely old" carbon reworked by glacial scouring of Tertiary sedimentary deposits during the Late
376 Glacial. In addition, McCulloch et al. (2005) have identified age offsets >10,000 ^{14}C years between
377 untreated (bulk) samples and >120 μm hand-picked macrofossil age determinations from sites along the
378 Bahía Inútil coastline on the eastern side of the Straits of Magellan (Figure 1). Similar to what we
379 identify in Lago Fagnano sediments, Heusser (1999) described the contaminant as, "black, amorphous,
380 noncrystalline, microscopic particulate without cellular differentiation." The Vandergoes and Prior
381 (2003) method used here has effectively eliminated these black particles from our samples and has
382 therefore allowed us to construct a working AMS radiocarbon chronology for Lago Fagnano. The results
383 from these two studies, as well as our own, indicate that contamination by radiocarbon "dead" carbon
384 derived from Tertiary sedimentary exposures is prevalent across Tierra del Fuego and should be kept in
385 mind when new regional radiocarbon chronologies are developed. Based on the radiocarbon evidence
386 presented here, our previous age models from Lago Fagnano that incorporate bulk or basal turbidite
387 organic matter should be considered suspect. The age model presented here reflects the most up-to-date
388 chronology for the Lago Fagnano eastern sub-basin and should be the chronology utilized in future work.

389 *5.2 Lago Fagnano sediment provenance*

390 Bulk organic C and N isotopic ratios and concentrations can be used to understand sediment
391 provenance, as well as transport and delivery mechanisms, within the Lago Fagnano watershed. C/N
392 ratios, for example, are commonly used to differentiate between algal and terrestrial sources of organic
393 matter in lacustrine sediments (Meyers and Teranes, 2001). Terrestrial organic matter derived from
394 vascular land plants with relatively high cellulose concentration and low protein abundance typically have
395 C/N ratios > 20 (Meyers, 2003). Conversely, lacustrine algae typically have C/N values < 10 due to
396 higher protein concentrations relative to land plants. Because lacustrine organic matter is typically a

mixture of terrestrial and aquatic organic matter, C/N ratios can be used to identify the relative contributions of these two end-members to the sediment (Meyers and Teranes, 2001). Figure 6 displays the bulk density, C/N ratio, and bulk $\delta^{13}C$ depth profiles for PC-18. With the exception of the large peak between 3 and 15 cm, C/N ratios are <10 throughout the record, indicating a predominantly algal source for the sedimentary organic matter. C/N ratios can also be combined with bulk density and $\delta^{13}C$ to highlight the turbidite deposits in the record (Figure 6). In Fagnano sediment cores, turbidites 2-8 are characterized by an initial increase in C/N ratio followed by a rapid drop and subsequent rise to pre-turbidite values (Figure 6). Synchronous decreases in $\delta^{13}C$ that begin with the initial rise in C/N and abrupt increases in bulk density clearly characterize these units and offer the potential to remove them from the sedimentary record (see below). The initial rise in C/N ratio and decline in $\delta^{13}C$ values probably reflect delivery of organic matter from littoral regions of the lake, while the low C/N values result from the fine-grained inorganic clays that cap the top of the turbidite unit (Figure 4). All terrestrial macrofossils found in the cores were obtained from the bases of these units, while the low C and N concentration clays are characterized as reflective light-colored layers in sediment core images (Figure 3). The large turbidite at the top of the record is different from the smaller turbidites found throughout the core. The concomitant rise in C/N ratio and bulk density is synchronous with a >0.5‰ decline in $\delta^{13}C$. Taken together, the data argue for large-scale downslope transport of terrestrial-derived organic matter. Waldmann et al. (2008) and Waldmann et al. (2010b) attribute turbidite deposition to tectonics-related mass flow events caused by seismicity along the Magallanes-Fagnano Transform fault system. We now expand upon this interpretation by combining bulk organic $\delta^{13}C$ and C/N measurements on representative organic material from Lago Fagnano and the surrounding watershed to constrain and identify locations of sediment supply to the deep eastern sub-basin.

In Figure 7 we compare $\delta^{13}C$ and C/N values from the PC-18 core and grab samples from the eastern sub-basin with terrestrial organic matter (soil, leaf litter, and *Nothofagus* leaves) from the surrounding watershed. PC-18 sediments were divided into non-turbidite (i.e., pelagic) and turbidite

categories based on the parameters presented in Figure 6 (bulk density, C/N ratio, and $\delta^{13}C$). Pelagic lacustrine sediments are well-constrained in the carbon cross-plot between -25.2 and -26 ‰ and 7.5 and 10 C/N units (Figure 7b). Lacustrine sediments derived from turbidite intervals also plot within the range of the pelagic sediments, but half of the measured values have lower C/N values, which can be attributed to the fine-grained inorganic clays that comprise the tops of these units and have low C and N concentrations (0.4% and 0.07%, respectively). The large turbidite at the top of the sediment core exhibits higher C/N values and lower $\delta^{13}C$ values and therefore plots separately from the pelagic sediments and other turbidite samples (Figure 7). In fact, this large turbidite exhibits C/N values close to those of grab samples obtained from shallower areas in the lake, and as a whole, plots within range of a shallow grab sample obtained close to the Río Turbio inlet. Therefore, this uppermost turbidite appears to contain organic matter derived from shallower or littoral areas of the lake, while the smaller turbidites (2-8, Figure 6) in the Holocene section appear to be sourced primarily from deeper sections of the sub-basin.

The relationship between water depth, distance from shore, and bulk $\delta^{13}C$ and C/N values is presented in Figure 8, where along E-W and N-S grab sample transects (see Figure 2b), $\delta^{13}C$ increases and C/N decreases with water depth. The large recent turbidite at the top of the PC-18 core may have been deposited as a result of collapse following a particularly large seismic event or slope failure during a moderate-sized, non-seismic event (e.g. gravitational delta collapse of some kind near the mouth of the Río Turbio). The smaller turbidites may reflect downslope-flows triggered by lower-magnitude seismic events that cause slope instabilities and thus mobilization and re-suspension of lacustrine sediments from lateral slopes, although the macrofossil samples found at the base of turbidites #3 and #5 also indicate some transport of littoral organic material. Finally, samples obtained from the top 3 cm of the PC-18 core (highlighted by the circle) and sediment grab samples may exhibit lower $\delta^{13}C$ values due to the 1.5‰ decline in atmospheric $\delta^{13}C$ CO_2 (Suess effect; Keeling, 1979; Schelske and Hodell, 1995).

5.3 Paleoclimate interpretation

446 Combining bulk organic geochemistry, the pollen-concentrate age model and knowledge of
447 sedimentation provided by the high-resolution seismic data from Lago Fagnano, allows us to draw
448 conclusions regarding past climate variability in Tierra del Fuego. In Figure 9 we present C/N, carbon
449 mass accumulation rates (C-MAR), and bulk organic $\delta^{13}C$ profiles for the last 8,000 years. We have
450 constructed these time series by incorporating the linear age model (Figure 5b) with the bulk geochemical
451 measurements obtained from the turbidite-free intervals (Figures 4 and 6). C/N and C-MAR co-vary and
452 show a rise through the Holocene that culminates in the last 500 years of the record (Figure 9a). The co-
453 variation of these two parameters suggests that higher carbon deposition rates result from higher fluxes of
454 terrestrial organic matter, either sourced from shallower areas (Figure 8) and/or from greater fluvial input
455 to the lake (Figure 7). Although C/N may be susceptible to degradation processes by selective removal of
456 labile C compounds over N through time (e.g. Meyers and Terranes, 2002), the C and N isotope profiles
457 from Lago Fagnano do not provide evidence of this. There are no significant trends towards positive
458 values (selective removal of the lighter isotope) in these two isotope profiles that would suggest there is
459 significant organic matter degradation. In addition to the increase in C/N and C accumulation rates
460 through the Holocene, there is a concomitant increase in magnetic susceptibility that mirrors the middle to
461 late Holocene trends in C/N and C-MAR (Figure 4). Together, these proxies indicate that there is an
462 overall increase in terrestrial organic matter and terrigenous material to the deep eastern sub-basin. The
463 Holocene trend in these parameters most likely represents a combination of vegetation dynamics related
464 to a Holocene advance of the *Nothofagus* (southern beech) forest into the lake water shed and the
465 associated increase in precipitation that drives forest expansion.
466 Heusser (2003) developed a pollen record from a mire located directly south of our coring sites
467 within the Lago Fagnano drainage basin. The record shows an increase in *Nothofagus* pollen from 9200
468 to 5500 cal yr BP that is followed by high *Nothofagus* percentages (>90 %) to modern. Because the
469 eastern limit of *Nothofagus* in this region is controlled by precipitation (Heusser, 1995; Heusser et al.,
470 2000; Huber et al. 2004; Markgraf et al., 2007; Tonello et al., 2009), the rise in *Nothofagus* pollen is
471 attributed to increasing moisture availability that expands and maintains the eastern extent of the forest

472 (Heusser, 2003). The predominance of *Nothofagus* over Poaceae (grasses) starting in the middle
473 Holocene and extending to Modern is a common feature of pollen records obtained from sites located
474 within the forest-steppe ecotone in southern Patagonia (Heusser, 1995; Huber et al., 2004; Markgraf and
475 Huber, 2010, Moreno et al., 2009a; Villa-Martinez and Moreno, 2007). Increasing C/N, C-MAR, and
476 magnetic susceptibility through the Holocene in our record likely reflects the combination of increased
477 precipitation and run-off combined with the establishment of a dense *Nothofagus* forest around the lake.
478 Because precipitation in this region is largely driven by the intensity of the Southern Hemisphere
479 westerly wind field (Garreaud, 2007; Moy et al., 2009), we interpret the increasing values of C/N, C-
480 MAR, and magnetic susceptibility through the mid-to-late Holocene as resulting from generally
481 increasing westerly wind strength at this latitude. Although our paleoclimate interpretation of C/N and C-
482 MAR agrees well with regional records (e.g. Huber et al., 2004, Markgraf et al., 2010, Moreno et al.,
483 2009), it is difficult to exclude an influence of long-term tectonic change or lake basin evolution on these
484 two parameters. If modern slip rates of 6 mm/year are maintained along the transform fault system during
485 the Holocene, there is potential for the northern side of the lake to move 50 meters relative to the southern
486 side over the length of our 8,000 year record. However, the shallow seismic stratigraphy indicates that
487 the sedimentary sequence surrounding PC-18 is relatively uniform and there is no evidence of large-scale
488 disturbance (Waldmann et al., 2008; Waldmann et al., 2010a).
489 The Holocene bulk organic $\delta^{13}C$ profile from Lago Fagnano increases at 8,000 cal yr BP, attains
490 high values between 7,000 and 5,000 cal yr BP, and gradually declines through the late Holocene (Figures
491 4 and 9). Although the total range in $\delta^{13}C$ is less than 1‰, the overall Holocene trend is similar to a
492 Holocene record of Antarctic air temperatures from the Taylor Dome ice core (Steig et al., 2000) and
493 reconstructed SST along the mid-latitude Chilean continental shelf (Lamy et al., 2002). These two
494 records generally exhibit higher temperatures during the early to middle Holocene between 7,000 and
495 5,000 cal yr BP, followed by a gradual decline through the Neogacial period (Porter, 2000) during the last
496 5,000 years (Figure 9). The Lago Fagnano $\delta^{13}C$ records exhibits a very similar structure over this time
497 period, and likely reflects temperature-driven changes in algal productivity within the lake. Increased

498 temperatures, particularly during the summer months, will work to enhance phytoplankton productivity in
499 Lago Fagnano, preferentially removing ^{12}C from the water TDIC pool leaving and producing organic
500 debris enriched in ^{13}C (Hodell and Schelske, 1998; Hollander and McKenzie, 1991). The highest $\delta^{13}C$
501 values in the Fagnano record between 7,000 and 5,000 cal yr BP are coincident with low C/N values and
502 the highest Si/C ratios of the Holocene (not shown), further suggesting that the mid Holocene $\delta^{13}C$ peak is
503 indeed related to enhanced aquatic productivity. The correspondence between these three records
504 indicates that the mid-Holocene warming was pervasive in the mid- to high-latitudes of the South
505 American sector of the South Pacific region and extended across the Drake Passage to the Antarctic
506 continent. In particular, this early to middle Holocene warming may represent a significant warming of
507 ACC waters and may represent a weakening or northward migration in the polar front during the middle
508 Holocene.

509 Although our bulk radiocarbon dates are contaminated by bedrock derived lignite, it is unlikely
510 that the lignite will have a significant impact on our Holocene $\delta^{13}C$ profile because: (1) coal exhibits high
511 C/N values >50 (Ussiri and Lal, 2008), which are significantly elevated above the C/N values in our cores
512 (Figure 4), and would suggest that the lignite is not an overwhelming part of the sedimentary matrix, (2)
513 the alkali pre-treatment for bulk sedimentary radiocarbon samples that we employed preferentially
514 removes the younger more labile carbon that is retained in the $\delta^{13}C$ measurement and works to
515 concentrate the "dead" more refractory carbon yielding older age measurements, and (3) the linear offset
516 between pollen and bulk ages (Figure 5) decreases towards Modern at the same time carbon
517 accumulation rates are increasing, which is opposite to what we would expect if bedrock-derived lignite is
518 significantly contributing to the bulk organic geochemical measurements. Regardless, future paleoclimate
519 work in Lago Fagnano will target compound-specific isotope methods (Huang et al., 2002; Shuman et al.,
520 2006; Tierney et al., 2008), which can be used to avoid contamination and get a better understanding of
521 Holocene changes in climate.
522

6. Conclusions

The Lago Fagnano sediment record provides a unique perspective on Holocene climate and tectonic disturbances in Tierra del Fuego. We have combined bulk C and N stable isotopic ratios and elemental analysis on a lacustrine sedimentary sequence recovered from Lago Fagnano to track changes in sediment provenance and aquatic productivity during the last 8,000 years. Although bedrock-derived lignite appears to be a significant radiocarbon contaminant in Lago Fagnano bulk organic sediments, radiocarbon dates obtained on pollen extracts provide a good chronology for the eastern sub-basin. Removing the influence of interpreted turbidites in the sedimentary record produces a linear age model for the last 8,000 years, and based on the reproducibility of radiocarbon dates and our interpolated age for the H1 tephra, we estimate our chronology to be accurate to 500 years or better during the Holocene. Future work on Lago Fagnano cored sediments will focus on reducing the uncertainty in the chronology by increasing the downcore density of pollen-concentrate radiocarbon dates.

Combining bulk elemental, isotopic, and physical sediment properties has allowed us to highlight the distribution in this part of the eastern sub-basin and better understand provenance associated with turbidites in the recovered sedimentary record. Turbidites 2-8 may reflect small-scale mass flow events that primarily transport resuspended lacustrine silts and clays derived from lower lateral slopes, while turbidites 1 and 9 may represent larger-scale, mass flow events that transport organic material from shallower regions of the lake, perhaps in response to exceptionally strong regional seismic disturbances. However, unconstrained changes in sediment source and turbidite preservation (e.g. Waldmann et al., 2010b) preclude a direct evaluation of past seismic magnitude given the data presented here. Ultimately, additional sediment cores and increasing the density of seismic data in the eastern sub-basin will be needed to corroborate these interpretations. The co-variability and long-term Holocene trend in C/N ratio and carbon accumulation rate reflects an overall increase in the delivery of terrestrial organic matter to Lago Fagnano. We attribute these variations to an overall increase in westerly-derived precipitation that drives the *Nothofagus* forest eastward and enhances run-off and fluvial input of terrestrial organic matter

549 to the lake. The correspondence between the Lago Fagnano bulk organic $\delta^{13}C$ record and other marine
550 and terrestrial records from the Southern Hemisphere is intriguing and suggests to us a shared response to
551 high latitude temperature change during the middle and late Holocene.

552 **7. Acknowledgements**

553 We would like to thank the scientific and general staff at the Centro Austral de Investigaciones Científicas
554 (CADIC) in Ushuaia, Argentina for their continued help and support during this project. We thank
555 Captains Jorge Ebling and Rafael Quezada for their assistance with R/V Neecho operations. In addition,
556 we thank Steffen Saustrup and Mark Wiederspahn of the Institute for Geophysics for their technical
557 assistance in the field. Funding for this research was provided by a U.S. National Science Foundation
558 (NSF) SGER grant to RBD, Swiss NSF awards (10 200021-100668/1 and 200020-111928/1) to DA, and
559 a National Geographic Society grant (CRE12 7705-04) to JAA. C. Moy gratefully acknowledges support
560 from a U.S. Dept. of Energy Global Change Education Program Graduate Fellowship, a Kerry Kelts
561 Award from the Limnogeology division of the Geological Society of America, and a Stanford University
562 McGee grant. A portion of this work was performed under the auspices of the U.S. Department of Energy
563 by Lawrence Livermore National Laboratory in part under Contract W-7405-Eng-48 and in part under
564 Contract DE-AC52-07NA27344.

565

566 **8. References**

567 Aravena, J.C., Lara, A., Wolodarsky-Franke, A., Villalba, R. and Cuq, E., 2002. Tree-ring growth
568 patterns and temperature reconstruction from *Nothofagus pumillo* (Fagaceae) forests at the upper tree line
569 of southern Chilean Patagonia. Rev. Chil. Hist. Nat. 75, 361-376.
570
571 Belkin, I.M. and Gordon, A.L., 1996. Southern Ocean fronts from the Greenwich meridian to Tasmania.
572 J. Geophys. Res. 101, 3675–3696.
573
574 Bertrand, S., Sterken, M., Vargas-Ramirez, L., De Batist, M., Vyverman, W., Lepoint, G. and Fagel, N.,
575 2009. Bulk organic geochemistry of sediments from Puyehue Lake and its watershed (Chile, 40°S):
576 Implications for paleoenvironmental reconstructions. Palaeogeogr. Palaeoclimatol. Palaeoecol.
577 doi:10.1016/j.palaeo.2009.03.012.
578

Björck, S. and Wohlfarth, B., 2001. ^{14}C chronostratigraphic techniques in paleolimnology, in: W.M. Last and J.P. Smol (Eds.), Tracking Environmental Change Using Lake Sediments Kluwer Academic Publishers, Dordrecht, pp. 205-245.

Boninsegna, J.A., Keegan, J., Jacoby, G.C., D'Arrigo, R. and Holmes, R.L., 1990. Dendrochronological studies in Tierra del Fuego, Argentina. Quat. S. Amer. Ant. Pen. 7, 305-327.

Brown, T.A., Nelson, D.E., Mathewes, R.W., Vogel, J.S. and Southon, J.R., 1989. Radiocarbon dating of pollen by accelerator mass spectrometry. Quat. Res. 32, 205-212.

Bujalesky, G.G., Heusser, C.J., Coronato, A.M., Roig, C.E. and Rabassa, J.O., 1997. Pleistocene glaciolacustrine sedimentation at Lago Fagnano, Andes of Tierra del Fuego, southernmost South America. Quat. Sci. Rev. 16, 767-778.

Chondrogianni, C., Ariztegui, D., Rolph, T., Juggins, S., Shemesh, A., Rietti-Shati, M., Niessen, F., Guilizzoni, P., Lami, A., McKenzie, J.A. and Oldfield, F., 2004. Millennial to interannual climate variability in the Mediterranean during the Last Glacial Maximum. Quat. Int. 122, 31-41.

Clapperton, C.M., Sugden, D.E., Kaufman, D.S. and McCulloch, R.D., 1995. The last glaciation in central Magellan strait, southernmost Chile. Quat. Res. 44, 133-148.

Croudace, I. W., Rindby, A., and Rothwell, R. G. 2006. ITRAX: description and evaluation of a new multi-function X-ray core scanner. Geological Society, London, Special Publications. 267, 51–63.

DeMaster, D.J., 1981. The Supply and accumulation of silica in the marine environment. Geochim. Cosmochim. Acta. 45, 1715-1732.

Faegri, K. and Iversen, J., 1989. Textbook of Pollen Analysis. John Wiley & Sons, London.

Garreaud, R., 2007. Precipitation and circulation covariability in the extratropics. J. Clim. 20, 4789-4797.

Garreaud, R., Vuille, M., Compagnucci, R. and Marengo, J., 2009. Present-day South American Climate. Palaeogeogr. Palaeoclimatol. Palaeoecol. 281, 180-195.

Haberzettl, T., Corbella, H., Fey, M., Janssen, S., Lücke, A., Mayr, C., Ohlendorf, C., Schäbitz, F., Schleser, G.H., Wille, M., Wulf, S. and Zolitschka, B., 2007. Lateglacial and Holocene wet-dry cycles in southern Patagonia: chronology, sedimentology and geochemistry of a lacustrine record from Laguna Portok Aike, Argentina. Holocene. 17, 297-310.

Heusser, C.J., 1995. Three Late Quaternary pollen diagrams from southern Patagonia and their paleoecological implications. Palaeogeogr. Palaeoclimatol. Palaeoecol. 118, 1-24.

Heusser, C.J., 1999. ^{14}C age of glaciation in Estrecho de Magallanes-Bahía Inútil, Chile. Radiocarbon. 41, 287-293.

Heusser, C.J., 2003. Ice age southern Andes: A chronicle of paleoecological events. Elsevier, Amsterdam.

Heusser, C.J., Heusser, L.E., Lowell, T.V., Moreira, A. and Moreira, S., 2000. Deglacial palaeoclimate at Puerto del Hambre, subantarctic Patagonia, Chile. J. Quat. Sci. 15, 101-114.

Heusser, C.J. and Rabassa, J., 1987. Cold climatic episode of Younger Dryas age in Tierra del Fuego. Nature. 328, 609-11.

Heusser, C.J. and Rabassa, J., 1995. Late Holocene forest-steppe interaction at Cabo San Pablo, Isla Grande de Tierra del Fuego, Argentina. Quat. S. Amer. Ant. Pen. 9, 173-182.

Hodell, D.A., Kanfoush, S.L., Shemesh, A., Crosta, X., Charles, C.D. and Guilderson, T.P., 2001. Abrupt Cooling of Antarctic Surface Waters and Sea Ice Expansion in the South Atlantic Sector of the Southern Ocean at 5000 cal yr B.P. Quat. Res. 56, 191-198.

Hodell, D.A. and Schelske, C.L., 1998. Production, sedimentation and isotopic composition of organic material in Lake Ontario. Limnol. Oceanogr. 43, 200-214.

Hollander, D.J. and McKenzie, J.A., 1991. CO_2 control on carbon-isotope fractionation during aqueous photosynthesis: A paleo-pCO_2 barometer Geology. 19, 929-932.

Huang, Y., Shuman, B., Wang, Y. and Webb, T., 2002. Hydrogen isotope ratios of palmitic acid in lacustrine sediments record late Quaternary climate variations. Geology. 30, 1103–1106.

Huber, U.M., Markgraf, V. and Schäbitz, F., 2004. Geographical and temporal trends in Late Quaternary fire histories of Fuego-Patagonia, South America. Quat. Sci. Rev. 23, 1079-1097.

Kaplan, M.R., Hulton, N.R.J.C., A., Rabassa, J.O., Stone, J.O., Kubik, P.W. and Freeman, S., 2007. Cosmogenic nuclide measurements in southernmost South America and implications for landscape change. Geomorphology. 87, 284-301.

Kaplan, M.R., Fogwill, C.J., Sugden, D.E., Hulton, N.R.J., Kubik, P.W. and Freeman, S.P.H.T., 2008. Southern Patagonian glacial chronology for the Last Glacial period and implications for Southern Ocean climate. Quat. Sci. Rev. 27, 284-294.

Keeling, C.D., 1979. The Suess effect: ^{13}Carbon-^{14}Carbon interrelations. Environ. Int. 2, 229-300.

Kuylenstierna, J.L., Rosqvist, G.C. and Holmlund, P., 1996. Late-Holocene glacier variations in the Cordillera Darwin, Tierra del Fuego. Holocene. 6, 353-358.

Lamy, F., Ruhlemann, C., Hebbeln, D. and Wefer, G., 2002. High- and low-latitude climate control on the position of the southern Peru-Chile Current during the Holocene. Paleoceanography. 17, 1028.

Le Quéré, C., Rodenbeck, C., Buitenhuis, E.T., Conway, T.J., Langenfelds, R., Gomez, A., Labuschagne, C., Ramonet, M., Nakazawa, T., Metzl, N., Gillet, N. and Heimann, M., 2007. Saturation of the Southern Ocean CO_2 Sink Due to Recent Climate Change. Science. 316, 1735-1738.

Lodolo, E., Menichetti, M., Bartole, R., Ben-Avraham, Z., Tassone, A. and Lippai, H., 2003. Magallanes-Fagnano continental transform fault (Tierra del Fuego, southernmost South America). Tectonics. 22, 1076.

Lovenduski, N.S., Gruber, N., Doney, S.C. and Lima, I.D., 2007. Enhanced CO_2 outgassing in the Southern Ocean from a positive phase of the Southern Annular Mode. Global Biogeochem. Cycles. 21, GB2026.

679 Löwemark, L., Chen, H.-F., Yang, T.-N., Kylander, M., Yu, E.-F., Hsu, Y.-W., Lee, T.-Q., Song, S.-R.,
680 and Jarvis, S. 2010. Normalizing XRF-scanner data: A cautionary note on the interpretation of high-
681 resolution records from organic-rich lakes. J. Asian Earth Sci.
682
683 Markgraf, V., 1993. Paleoenvironments and paleoclimates in Tierra del Fuego and southernmost
684 Patagonia, South America. Palaeogeogr. Palaeoclimatol. Palaeoecol. 102, 53-68.
685
686 Markgraf, V., Whitlock, C., and Haberle, S. 2007. Vegetation and fire history during the last 18,000 cal yr
687 B.P. in Southern Patagonia: Mallín Pollux, Coyhaique, Province Aisén (45°41'30" S, 71°50'30" W, 640 m
688 elevation). Palaeogeogr. Palaeoclimatol. Palaeoecol. 254, 492-507.
689
690 Markgraf, V., and Huber, U. M. 2010. Late and postglacial vegetation and fire history in Southern
691 Patagonia and Tierra del Fuego. Palaeogeogr. Palaeoclimatol. Palaeoecol. 297, 351-366.
692
693 Mauquoy, D., Blaauw, M., van Geel, B., Borromei, A., Quattrocchio, M., Chambers, F. and Possnert, G.,
694 2004. Late Holocene climate changes in Tierra del Fuego based on multiproxy analyses of peat deposits.
695 Quat. Res. 61, 148-158.
696
697 Mayr, C., Fey, M., Haberzettl, T., Janssen, S., Lücke, A., Maidana, N., Ohlendorf, C., Schäbitz, F.,
698 Schleser, G.H., Struck, U., Wille, M. and Zolitschka, B., 2005. Palaeoenvironmental changes in southern
699 Patagonia during the last millennium recorded in lake sediments from Laguna Azul (Argentina).
700 Palaeogeogr. Palaeoclimatol. Palaeoecol. 228, 203-227.
701
702 McCormac, F.G., Hogg, A.G., Blackwell, P.G., Buck, C.E., Higham, T.F.G. and Reimer, P.J., 2004.
703 SHCal04 Southern Hemisphere Calibration 0 - 11.0 cal kyr BP. Radiocarbon. 46, 1087-1092.
704
705 McCulloch, R.D. and Bentley, M.J., 1998. Late Glacial ice advances in the Strait of Magellan, southern
706 Chile. Quat. Sci. Rev. 17, 775-87.
707
708 McCulloch, R.D., Fogwill, C.J., Sugden, D.E., Bentley, M.J. and Kubik, P.W., 2005. Chronology of the
709 last glaciation in central strait of Magellan and Bahia Inutil, southernmost South America. Geogr. Ann.
710 Ser. A. 87, 289-312.
711
712 Menichetti, M., Lodolo, E. and Tassone, A., 2008. Structural geology of the Fuegian Andes and
713 Magallane fold-and-thrust belt – Tierra del Fuego Island. Geol. Acta. 6, 19-42.
714
715 Mensing, S. and Southon, J.R., 1999. A simple method to separate pollen for AMS radiocarbon dating
716 and its application to lacustrine and marine sediments. Radiocarbon. 41, 1-8.
717
718 Mercer, J.H., 1982. Holocene glacial variations in southern South America. Striae. 18, 35-40.
719
720 Meyers, P.A., 2003. Applications of organic geochemistry to paleolimnological reconstructions: a
721 summary of examples from the Laurentian Great Lakes. Org. Geochem. 34, 261-289.
722
723 Meyers, P.A. and Teranes, J.L., 2001. Sediment organic matter, in: W.M. Last and J.P. Smol (Eds.),
724 Tracking Environmental Change Using Lake Sediments. Volume 2: Physical and Geochemical Methods.
725 Kluwer Academic Publishers, Dordrecht, The Netherlands, 239-270.
726
727 Moreno, P.I., Francois, J.P., Villa-Martinez, R. and Moy, C.M., 2009a. Millennial-scale variability in
728 Southern Hemisphere westerly wind activity over the last 5000 years in SW Patagonia. Quat. Sci. Rev.
729 28, 25-38.

Moreno, P.I., Kaplan, M.R., Francois, J.P., Villa-Martínez, R., Moy, C.M., Stern, C.R. and Kubik, P.W., 2009b. Renewed glacial activity during the Antarctic cold reversal and persistence of cold conditions until 11.5 ka in southwestern Patagonia. Geology. 37, 375-378.

Mortlock, R.A. and Froelich, P.N., 1989. A Simple Method for the Rapid Determination of Biogenic Opal in Pelagic Marine Sediments. Deep Sea Res. Part I Oceanogr. Res. Pap. 36, 1415-1426.

Moy, C.M., Dunbar, R.B., Moreno, P., Francois, J.P., Villa-Martinez, R., Guilderson, T.P. and Garreaud, R.D., 2008. Isotopic evidence for hydrologic change related to the westerlies in SW Patagonia, Chile, during the last millennium. Quat. Sci. Rev. 27, 1335-1349.

Moy, C.M., Moreno, P.I., Dunbar, R.B., Francois, J.P., Kaplan, M.R., Villalba, R. and Haberzettl, T., 2009. Climate change in southern South America during the last two millennia, in: F. Vimeux, F. Sylvestre and M. Khodri (Eds.), Past Climate Variability in South America and Surrounding Regions: From the Last Glacial Maximum to the Holocene. Springer Netherlands, 353-393.

Nielsen, S.H.H., Koc, N. and Crosta, X., 2004. Holocene climate in the Atlantic sector of the Southern Ocean: Controlled by insolation or oceanic circulation? Geology. 32, 317-320.

Olivero, E.B. and Malumián, N., 2008. Mesozoic-Cenozoic stratigraphy of the Fuegian Andes, Argentina. Geol. Acta. 6, 5-18.

Olsson, I., 1991. Accuracy and precision in sediment chronology. Hydrobiologia. 214, 25-34.

Pendall, E., Markgraf, V., White, J.W.C. and Dreier, M., 2001. Multiproxy record of Late Pleistocene-Holocene climate and vegetation changes from a peat bog in Patagonia. Quat. Res. 55, 168-178.

Piotrowska, N., Bluszcz, A., Demske, D., Granoszewski, W. and Heumann, G., 2004. Extraction and AMS radiocarbon dating of pollen from Lake Baikal sediments. Radiocarbon. 46, 181-187.

Porter, S.C., 2000. Onset of Neoglaciation in the Southern Hemisphere. J. Quat. Sci. 15, 395-408.

Rowe, H.D., Guilderson, T.P., Dunbar, R.B., Southon, J.R., Seltzer, G.O., Mucciarone, D.A., Fritz, S.C. and Baker, P.A., 2003. Late Quaternary lake-level changes constrained by radiocarbon and stable isotope studies on sediment cores from Lake Titicaca, South America. Glob. Planet. Change. 38, 273-290.

Sapkota, A., Cheburkin, A.K., Bonani, G. and Shotyk, W., 2007. Six millenia of atmospheric dust deposition in southern South America (Isla Navarino, Chile). The Holocene. 17, 561-572.

Schelske, C.L. and Hodell, D.A., 1995. Using carbon isotopes of bulk sedimentary organic matter to reconstruct the history of nutrient loading and eutrophication in Lake Eire. Limnol. Oceanogr. 40, 918-929.

Schnellmann, M., Anselmetti, F.S., Giardini, D. and McKenzie, J.A., 2005. Mass movement-induced fold-and-thrust belt structures in unconsolidated sediments in Lake Lucerne (Switzerland). Sedimentology. 52, 271-289.

Shuman, B., Huang, Y., Newby, P. and Wang, Y., 2006. Compound-specific isotopic analyses track changes in seasonal precipitation regimes in the Northeastern United States at ca 8200 cal yr BP. Quat. Sci. Rev. 26, 2992-3002.

Smalley, R., Kendrick, E., Bevis, M.G., Dalziel, I.W.D., Taylor, F., Lautia, E., Barriga, R., Casassa, G., Olivero, E.B. and Piana, E., 2003. Geodetic determination of relative plate motion and crustal deformation across the Scotia-South America plate boundary in eastern Tierra del Fuego. Geochem. Geophys. Geosyst. 4, 1070.

Steig, E.J., Morse, D.L., Waddington, E.D., Stuiver, M., Grootes, P.M., Mayewski, P.A., Twickler, M.S. and Whitlow, S.I., 2000. Wisconsinan and Holocene climate history from an ice core at Taylor Dome, Western Ross Embayment, Antarctica. Geogr. Ann. Ser. A. 82, 213-235.

Stern, C.R., 2008. Holocene tephrochronology record of large explosive eruptions in the southernmost Patagonian Andes. Bull. Volcanol. 70, 435-454.

Strelin, J. and Iturraspe, R., 2007. Recent evolution and mass balance of Cordón Martial glaciers, Cordillera Fueguina Oriental. Glob. Planet. Change. 59, 17-26.

Stuiver, M. and Reimer, P.J., 1993. Extended ^{14}C database and revised CALIB radiocarbon calibration program (version 6). Radiocarbon. 35, 215-230.

Tierney, J.E., Russell, J.M., Huang, Y., Sinninghe Damsté, J.S., Hopmans, E.C. and Cohen, A.S., 2008. Northern Hemisphere Controls on Tropical Southeast African Climate During the Past 60,000 Years. Science. 322, 252-255.

Toggweiler, J.R., Russell, J.L. and Carson, S.R., 2006. Midlatitude westerlies, atmospheric CO_2, and climate change during the ice ages. Paleoceanography. 21, PA2005.

Tonello, M. S., Mancini, M. V., and Seppä, H. 2009. Quantitative reconstruction of Holocene precipitation changes in southern Patagonia. Quat. Res. 72, 410-420.

Ussiri, D.A.N. and Lal, R., 2008. Method for determining coal carbon in the reclaimed minesoils contaminated with coal. Soil Sci. Soc. Am. J. 72, 231-237.

van Beek, P., Reyss, J.L., Paterne, M., Gersonde, R., van der Loeff, M.R. and Kuhn, G., 2002. ^{226}Ra in barite: Absolute dating of Holocene Southern Ocean sediments and reconstruction of sea-surface reservoir ages. Geology. 30, 731–734.

Vandergoes, M.J. and Prior, C.A., 2003. AMS dating of pollen concentrates-A methodological study of late Quaternary sediments from South Westland, New Zealand. Radiocarbon. 45, 479-491.

Villa-Martinez, R. and Moreno, P.I., 2007. Pollen evidence for variations in the southern margin of the westerly winds in SW Patagonia over the last 12,600 years. Quat. Res. 68, 400-409.

Waldmann, N., Ariztegui, D., Anselmetti, F.S., Austin, J.A., Dunbar, R., Moy, C.M. and Recasens, C., 2008. Seismic stratigraphy of Lago Fagnano sediments (Tierra del Fuego, Argentina) - A potential archive of paleoclimatic change and tectonic activity since the Late Glacial. Geol. Acta. 6, 101-110.

Waldmann, N., Ariztegui, D., Anselmetti, F.S., Austin, J.A., Stern, C., Moy, C.M., Recasens, C. and Dunbar, R., 2010a. Holocene climatic fluctuations and positioning of the Southern Hemisphere westerlies in Tierra del Fuego (54º S), Patagonia. J. Quat. Sci. 25, 1063-1075.

Waldmann, N., Anselmetti, F.S., Ariztegui, D., Austin, J.A., Pirouz, M., Moy, C.M. and Dunbar, R.,

2010b. Holocene mass-wasting events in Lago Fagnano, Tierra del Fuego (54°S): Implications for paleoseismicity of the Magallanes-Fagnano transform fault. Basin Research. doi: 10.1111/j.1365-2117.2010.00489.x.

835

836 **Figure Captions:**

837 Figure 1. Regional study area map illustrating location of Lago Fagnano and sites discussed in text. a)
838 Map of southern South America showing the location of Volcán Hudson (triangle) and the location of the
839 Heusser (1999) and McCulloch et al., (2005) site locations (numbered #1 and #2, respectively). Star
840 denotes the location of Lago Fagnano. b) Satellite image of Lago Fagnano and surrounding drainage
841 basin. Numbered stars denote the location of the PC-18 (1) and LF01 (2) sediment cores obtained in the
842 eastern basin. The circle denotes the location of the Lago Fagnano meteorological station and the white
843 box highlights the area enlarged in Figure 2a. Landsat image source: NASA World Wind
844 (http://worldwind.arc.nasa.gov).

845

846 Figure 2. Lago Fagnano bathymetry and seismic stratigraphy showing sediment core and grab sample
847 locations discussed in text. a) Lago Fagnano bathymetric map and seismic track lines for the western (W)
848 and eastern sub-basins (E). b) Eastern sub-basin bathymetry piston and gravity core locations (stars) and
849 the N-S and E-W grab sample transects (circles). In this paper, we focus on the PC-18 sediment record
850 obtained from 185 meters water depth and close to E-W seismic line #17 (labeled 2C). c) High resolution
851 3.6 kHz single-channel "pinger" seismic line #17 showing a longitudinal image of the eastern sub-basin
852 (the closest and most representative line for core PC-18) and the transposed location of PC-18. The PC-
853 18 record exposes the upper portion of the EC seismic stratigraphic unit, which is characterized by thinly
854 spaced, high-amplitude internal reflections with low-amplitude to transparent intervals. The EC unit has
855 been interpreted to reflect pelagic/lacustrine conditions interbedded with downslope mass-flow events
856 (Waldmann et al., 2010a). The geochemical record presented here focuses on the uppermost 230 cm of
857 this sequence.

858

859 Figure 3. Lago Fagnano PC-18 piston core composite linescan image. The upper core image (0 - 130
860 cm) highlights the core-top, a representative laminated interval, and turbidite #3 (note white inorganic

clay unit that caps this deposit). The lower core image highlights the erosive transition from the upper undisturbed section (top 230 cm) to the disturbed section below. Note the presence of a 7 cm-thick sandy turbidite at the base of the undisturbed section, multiple erosive boundaries, graded sequences, deformation structures, and the location of the V. Hudson (H1) tephra.

Figure 4. Compilation of Lago Fagnano bulk organic proxies. Numbers 1 – 9 and horizontal shading highlight interpreted turbidites in the record (as determined by visual inspection, e.g. Figure 3), which are characterized by abrupt drops in C and N concentrations, C/N, and $\delta^{13}C$. Triangles refer to pollen concentrate radiocarbon dates used in our age model and the dark heavy horizontal line shows the location of the H1 tephra within the disturbed (hatched) interval. Our paleoclimate interpretation is restricted to the upper 230 cm of the sediment core stratigraphy.

Figure 5. Radiocarbon chronology for the Lago Fagnano PC-18 sediment core. a) Age-depth (unmodified) profile for the PC-18 core showing dates obtained on pollen concentrates (circles), bulk sediment (diamonds), and terrestrial macrofossils (triangles). Pollen concentrates are younger than corresponding bulk sediment dates and exhibit a linear downcore distribution without any age reversals. b) Age-depth profile for the modified stratigraphy (interpreted turbidites removed) showing linear regression through pollen concentrates used as an age model for the PC-18 core. Although there is uncertainty in the placement or true depth of the H1 tephra in our cores due to its presence within the turbidite, our age model approximates the published age of the tephra within 400 years and provides another estimate of the accuracy of our chronology.

Figure 6. Lago Fagnano bulk organic and bulk density stratigraphy illustrating turbidite distribution within the record. We have removed the highlighted turbidites (1-9) from the bulk organic stratigraphy in order to interpret the paleoclimate record.

Figure 7. Cross plots of $\delta^{13}C$ and C/N illustrating potential Lago Fagnano sedimentary organic matter sources. a) Compilation of $\delta^{13}C$ and C/N measurements made on drainage basin organic matter (soil and

885 leaf litter) and lacustrine sediments obtained on the PC-18 sediment core and from grab samples obtained
886 along a N-S and E-W transect across the eastern basin (see Figure 2b). The terrestrial and sediment grab
887 samples plot along a mixing line between PC-18 sediment samples and a terrestrial end-member best
888 represented by leaf litter. b) Same as in 7a but enlarged to show variations between PC-18 sediment core
889 samples and grab samples. The grab samples trend along a curved line extending from a shallow sample
890 obtained close to the Río Turbio inlet to the PC-18 samples obtained from the largest turbidite (Turbidite
891 1). The Turbidite 1 samples exhibit higher C/N values and therefore plot away from the other turbidite
892 and non-turbidite PC-18 samples. Grab samples and the top 3cm PC-18 samples may be artificially
893 depressed by ~1‰ due to the Suess effect (1.5‰ decline in atmospheric $\delta^{13}C$ due to combustion of
894 isotopically light fossil fuels; see text).

895 Figure 8. Grab sample C/N and $\delta^{13}C$ plotted as a function of water depth. C/N increases and $\delta^{13}C$
896 generally decreases in grab samples obtained closer to shore at shallower water depths.

897 Figure 9. Compilation of Lago Fagnano paleoclimate proxies and selected Southern Hemisphere
898 paleoclimate records. a) Co-variability and the increasing Holocene trend in C/N and C-MAR provide
899 evidence for enhanced drainage basin erosion and expansion of the *Nothofagus* forest around the lake
900 during the last 8,000 years due to an increase in westerly-derived precipitation. b) Alkenone SST
901 reconstruction from the Chilean continental margin (41°S; Lamy et al., 2002). c) $\delta^{13}C$ profile from Lago
902 Fagnano (this study). The $\delta^{13}C$ profile provides evidence for enhanced aquatic productivity during the
903 mid Holocene between 7,000 and 5,000 cal yr BP that likely reflects warmer summer temperatures. After
904 5,000 cal yr BP both profiles decline toward present and may reflect cooler summer temperatures related
905 with Neoglacial ice expansion in the region after 5,500 cal yr BP (Porter, 2000). d) The Taylor Dome δD
906 record (Steig et al., 2000) exhibits a similar Holocene profile to the Lago Fagnano record: an early
907 Holocene warming is evident between 7,000 and 6,000 cal yr BP, which is followed by a gradual cooling
908 through the Neoglacial period towards Present.

Table 1. Summary of radiocarbon dates obtained from Lago Fagnano bulk sediments, pollen concentrates and terrestrial macrofossils.

Supplementary Figure Captions:

Supplemental Figure 1. Meteorological composites derived from the Lago Fagnano weather station. a) Wind rose diagram illustrating relative frequency distribution of wind direction and speed from 2004 to 2008. The rose diagram indicates that the predominant wind direction is out of the SW, but higher wind velocities can also originate from the WNW and NW. b) Monthly meteorological composites of temperature, wind speed and precipitation obtained from Lago Fagnano and Ushuaia (precipitation) from 2004 to 2008.

Supplemental Figure 2. Compilation of bulk density profiles obtained from Lago Fagnano eastern sub-basin piston and gravity cores. The nine Holocene interpreted turbidite deposits are characterized by abrupt increases in bulk density and can be traced across multiple sediment cores. We have used the bulk density profiles to transfer radiocarbon ages from LF01 to the PC-18 sediment cores. Inset diagram shows eastern sub-basin bathymetry from Figure 2b.

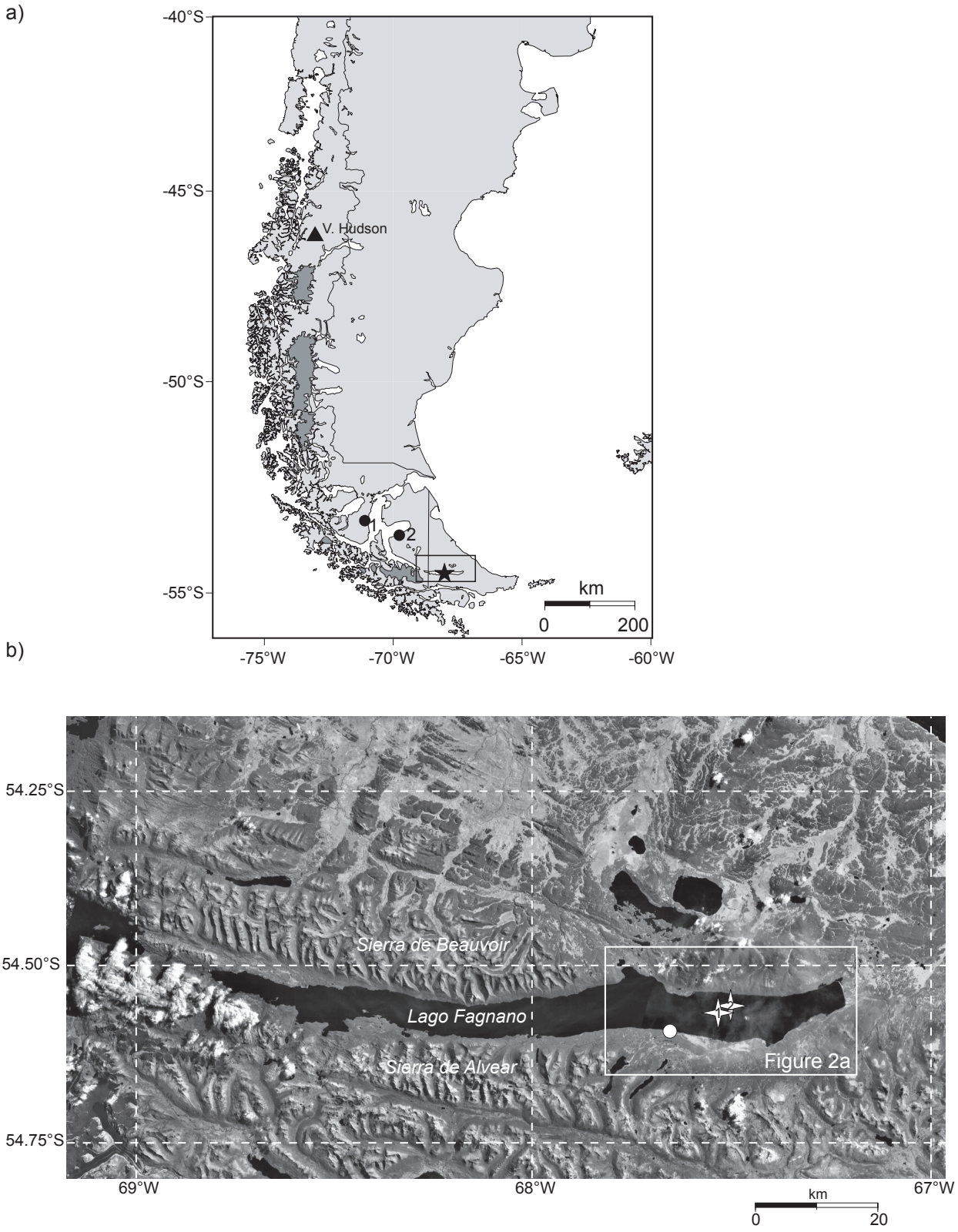

Figure 1 - online & print version

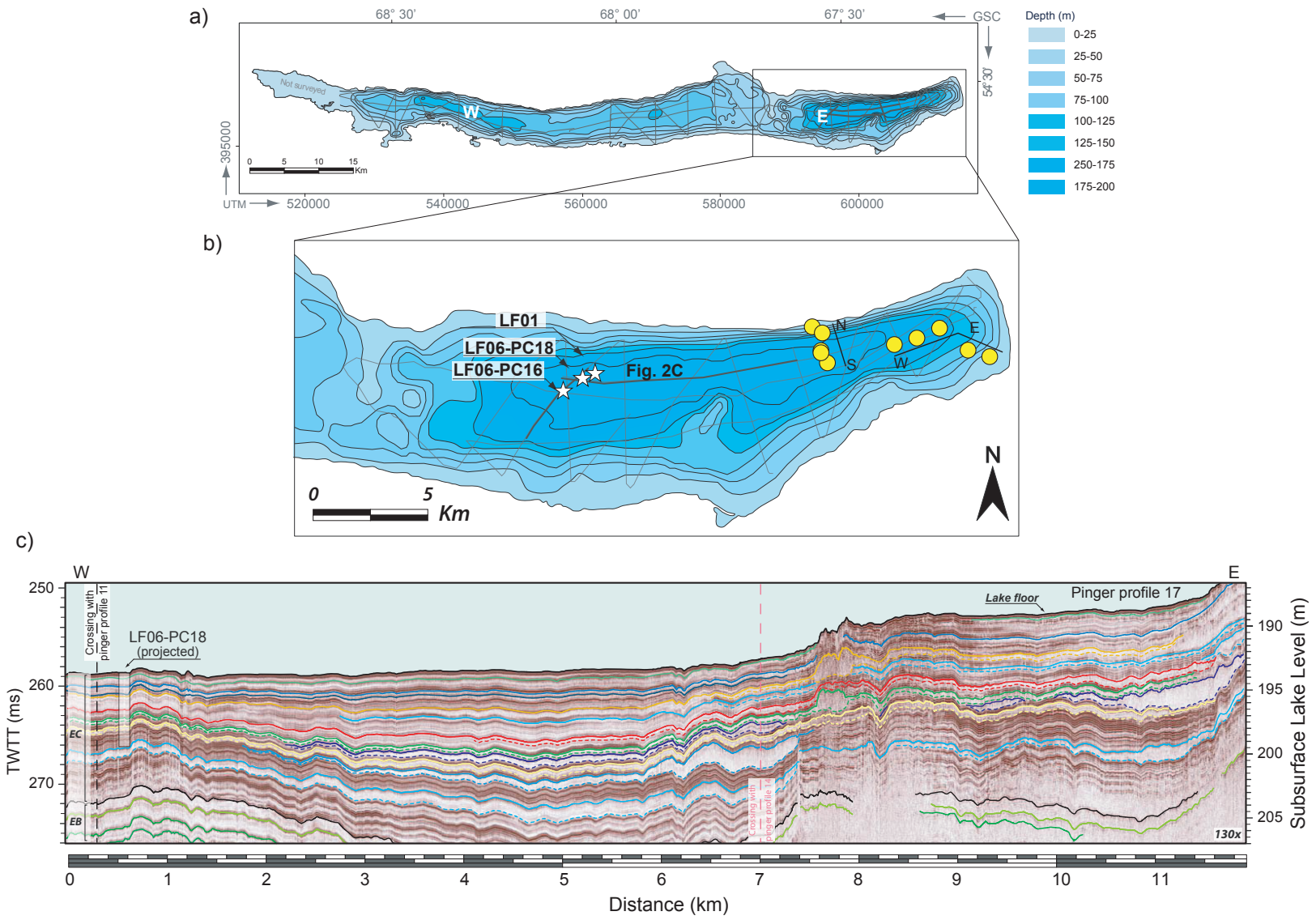

Figure 2 - online version

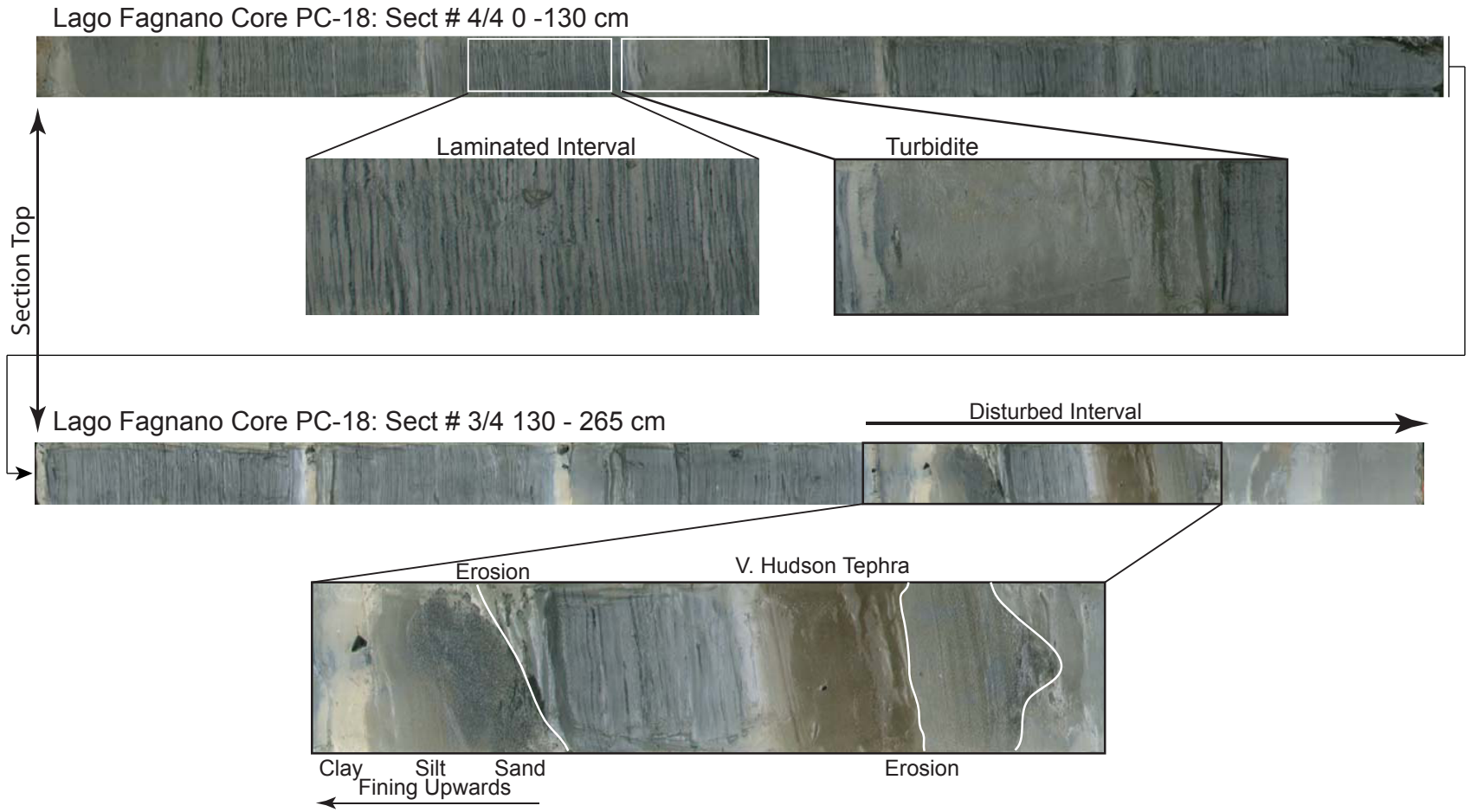

Figure 3 - online version

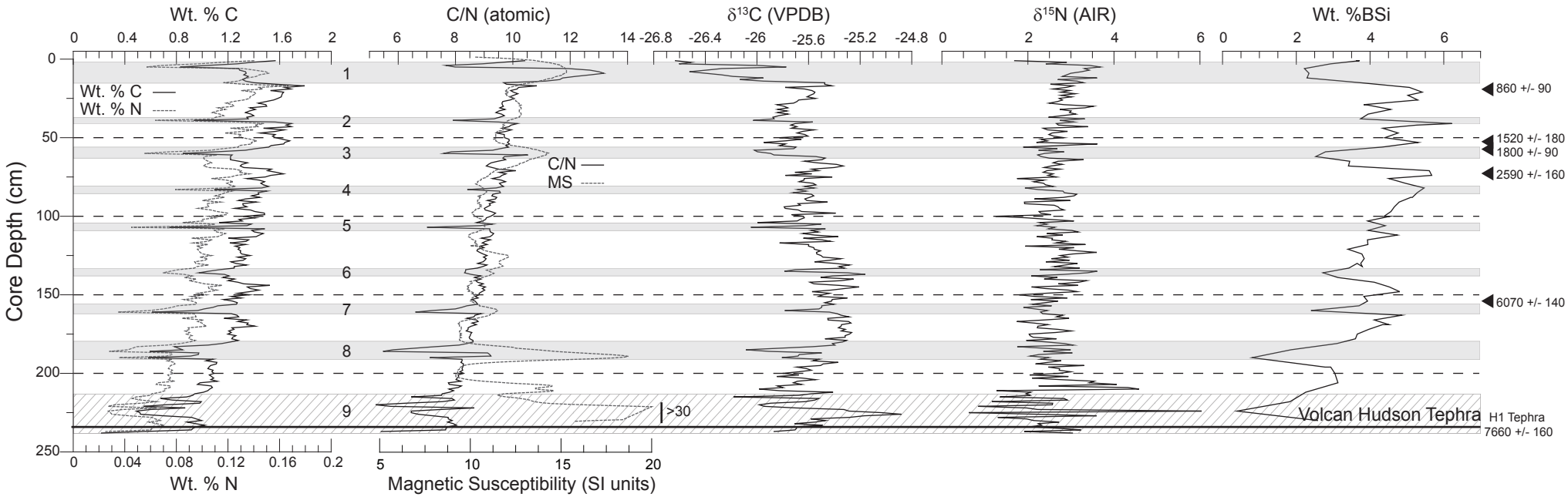

Figure 4 - online and print version

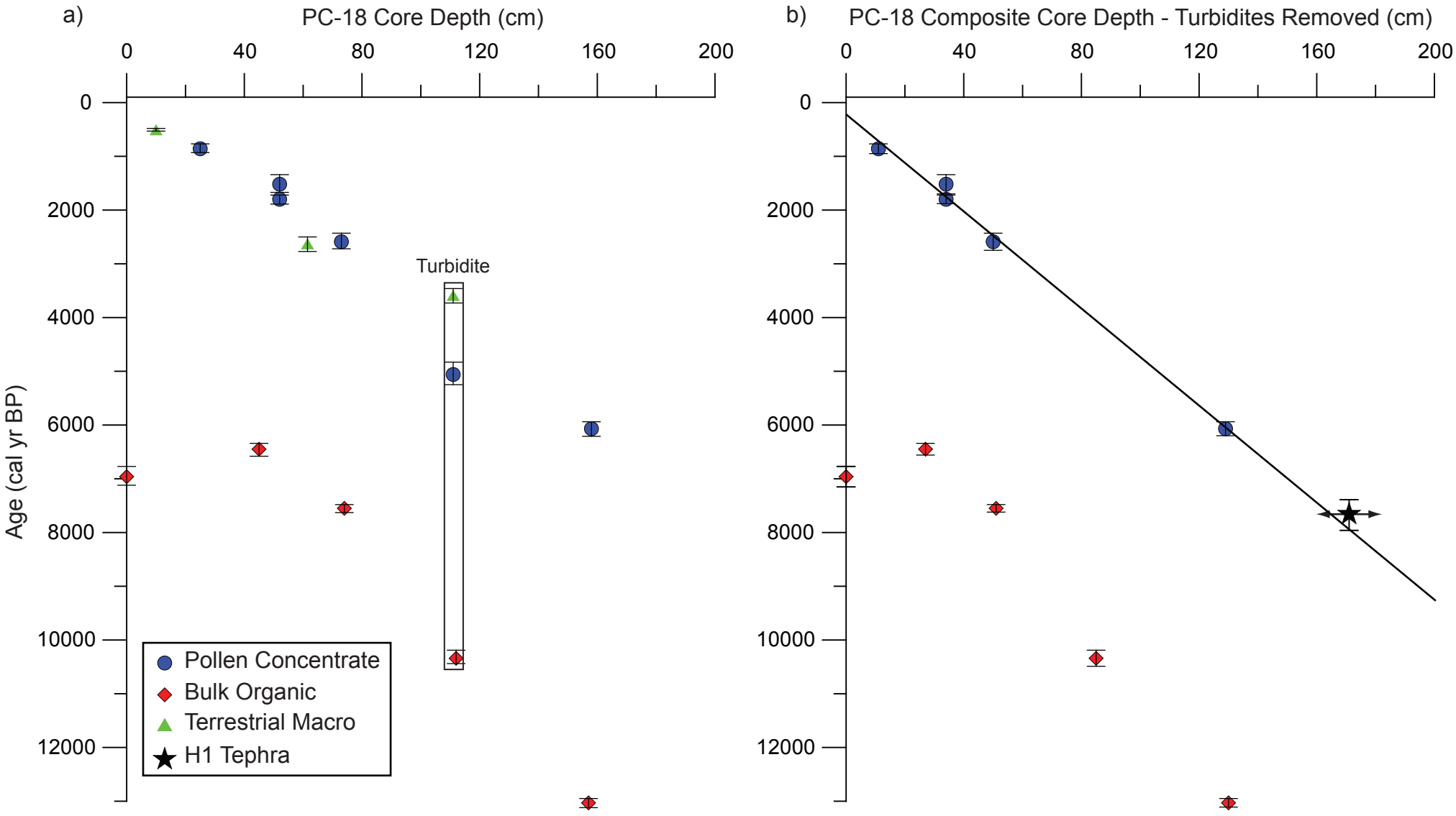

Figure 5 - online version

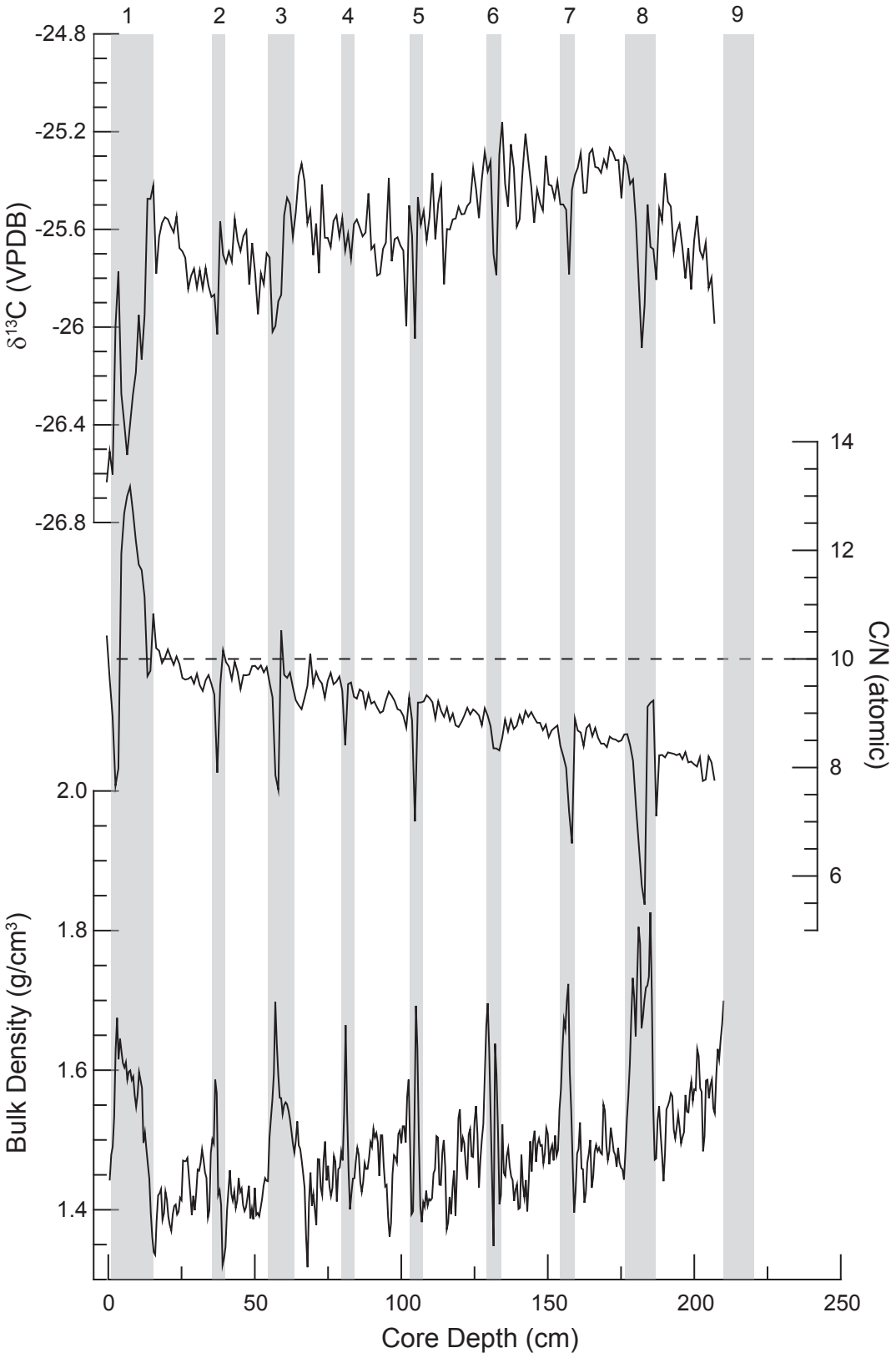

Figure 6 - online & print version

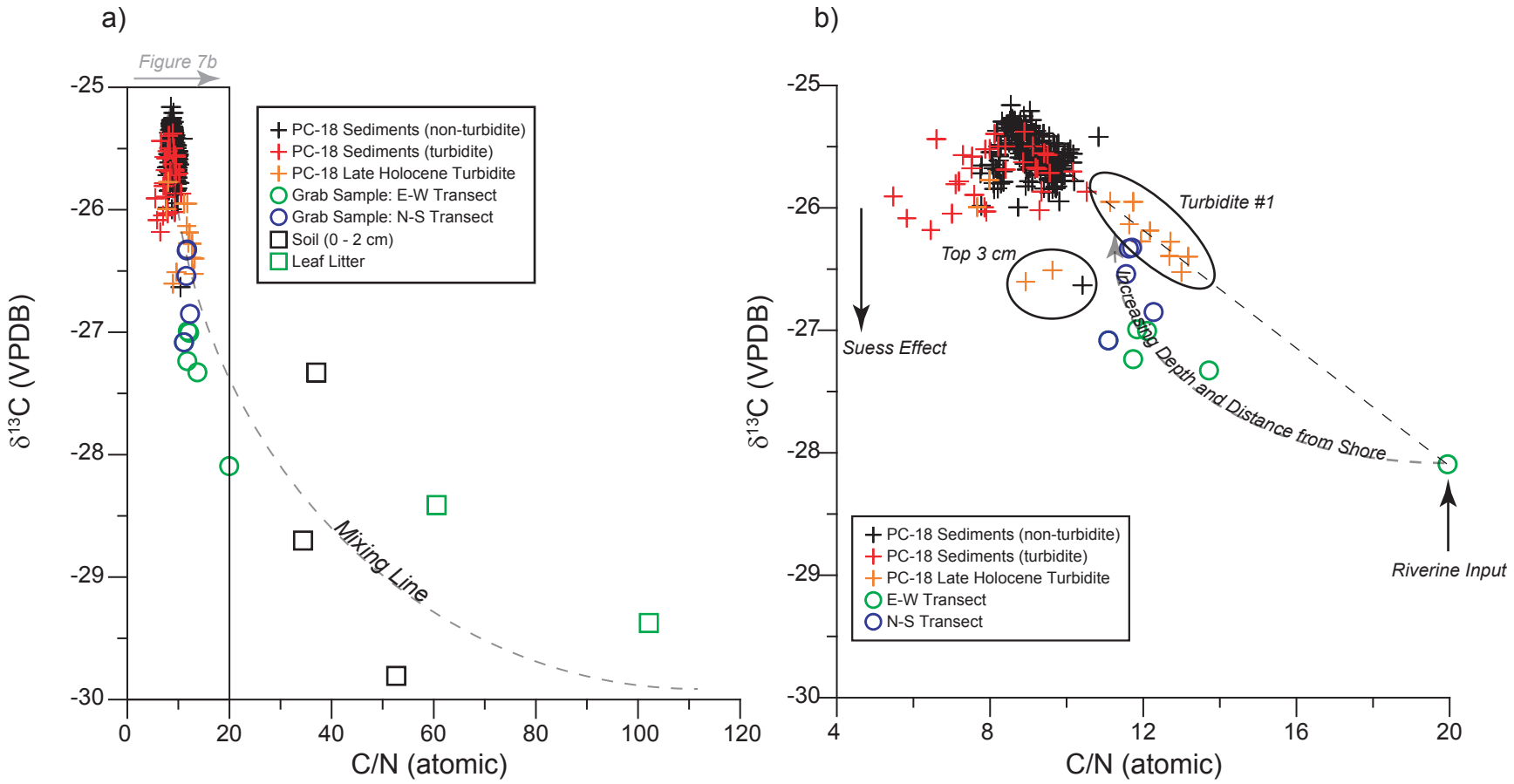

Figure 7 - online version

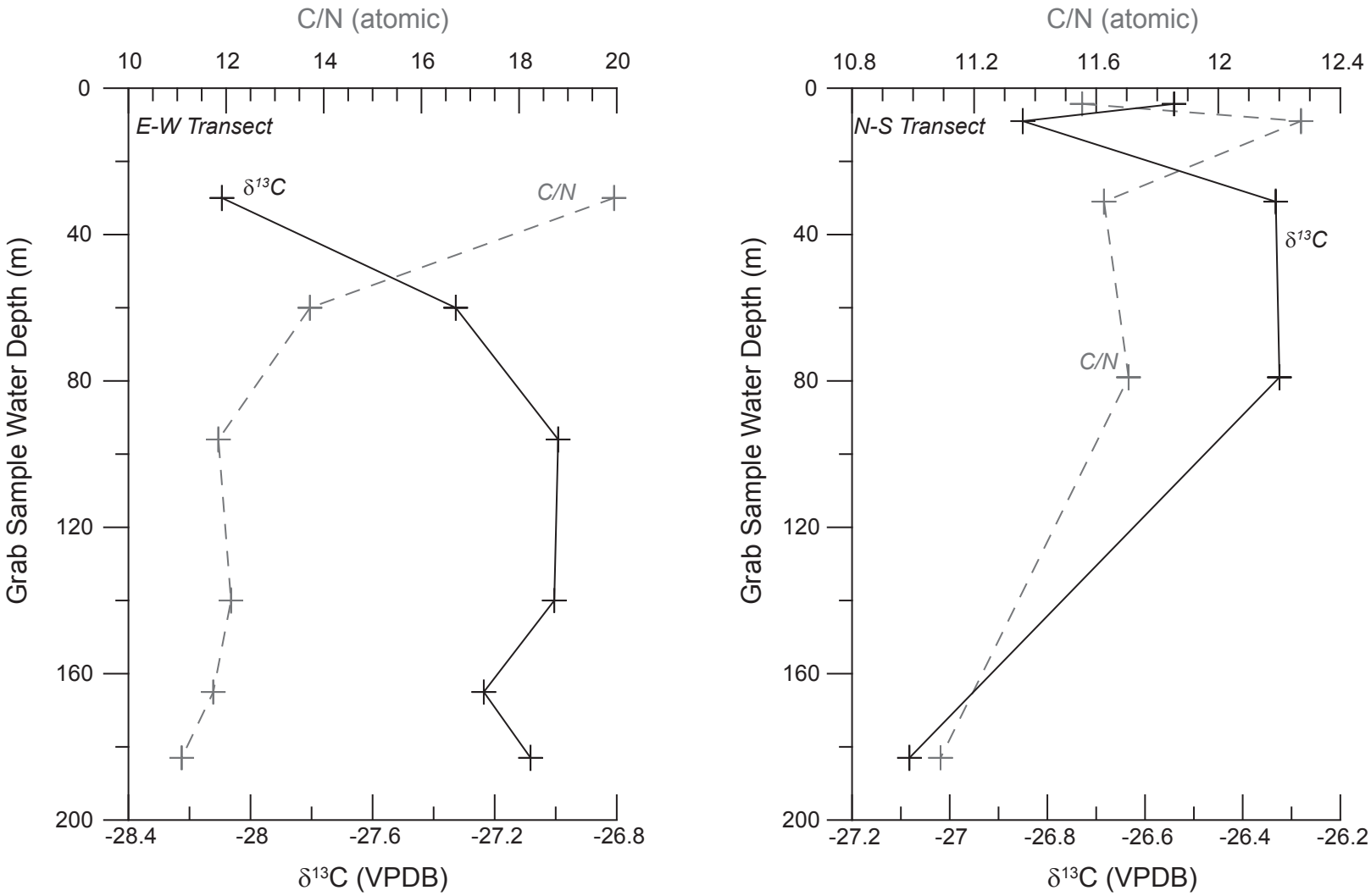

Figure 8 - online & print version

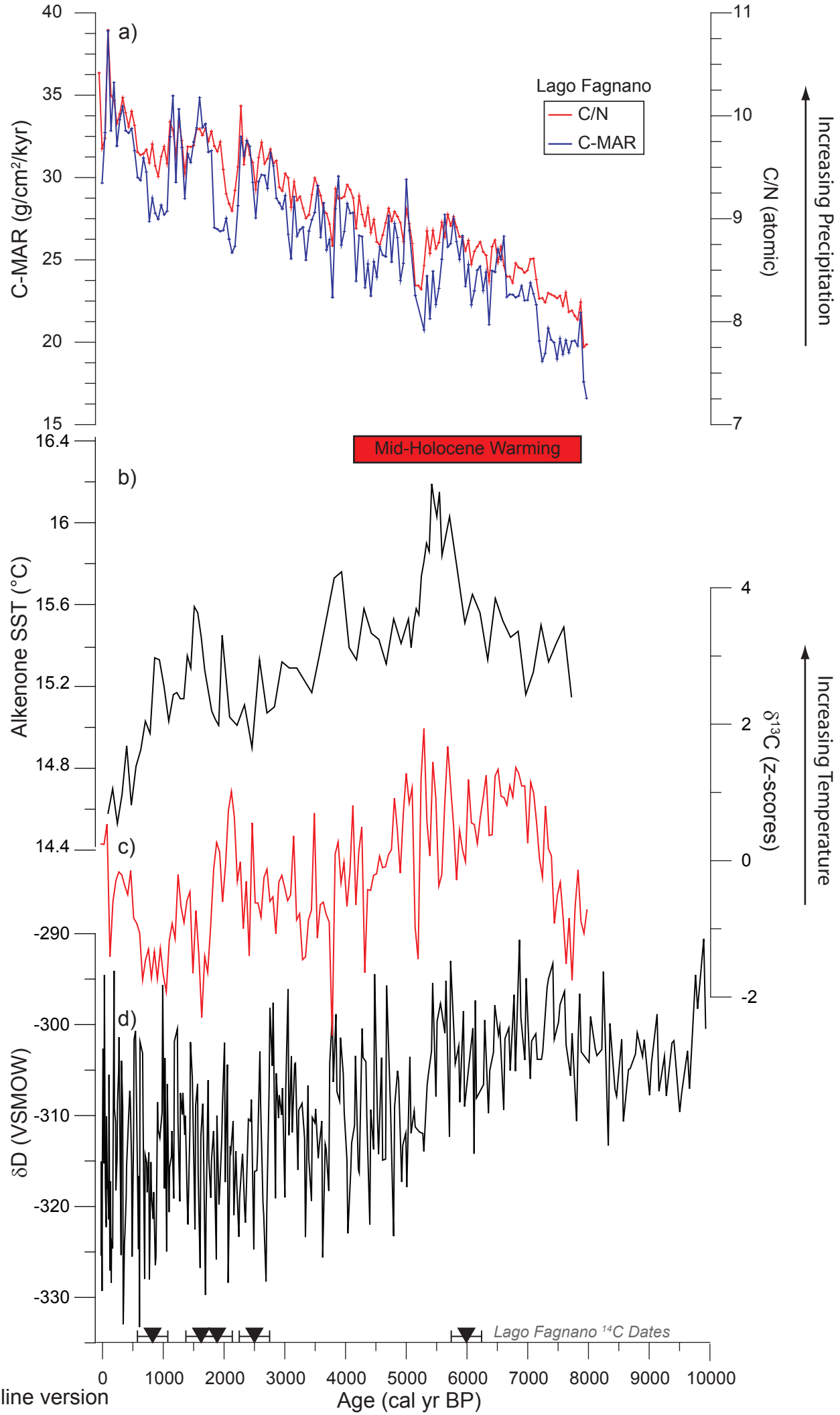

Figure 9 - online version

#	CAMS #	Sample ID	Core	Core Depth (cm)	PC-18 Composite Depth (cm)	Modified Depth -- Turbidites removed (cm)	Material	Age	Error	Median Probability Age (cal yr BP)	2σ lower	2σ upper
1	115796	LF01_0	LF01	0	0	0	Bulk Organic	6150	30	6960	160	190
2	115797	LF01_57.5	LF01	57.5	45	27	Bulk Organic	5720	35	6450	130	110
3	115798	LF01_92.5	LF01	92.5	74	51	Bulk Organic	6740	35	7550	80	70
4	115799	LF01_154.5	LF01	154.5	112	85	Bulk Organic	9235	35	10340	100	150
5	115800	LF01_227.5	LF01	227.5	157	130	Bulk Organic	11125	35	13030	90	80
6	118297	LF01 22	LF01	22	25	11	Pollen- 1.6 g/cm^3	1015	35	860	70	90
7	118298	LF01 65	LF01	65	52	34	Pollen- 1.6 g/cm^3	1920	30	1800	90	80
8	118366	LF01_65_1.3	LF01	65	52	34	Pollen- 1.3 g/cm^3	1680	70	1520	150	180
9	118364	LF01_91	LF01	91	73	50	Pollen- 1.6 gm/cm^3	2565	35	2590	130	160
10	118365	LF01_153	LF01	153	111	84	Pollen- 1.6 gm/cm^3	4495	50	5060	190	230
11	118366	LF01_227.5_1.4	LF01	227	158	129	Pollen- 1.6 gm/cm^3	5335	50	6070	140	130
12	118367	LF01_153_wood	LF01	153	111	84	Terrestrial Macro	3410	50	3590	140	130
13	128995	LF06_sect4_10	PC-18	10	10	-	Terrestrial Macro	505	35	510	20	30
14	128996	LFO6_sect4_61.5	PC-18	61.5	61.5	-	Terrestrial Macro	2610	35	2630	140	130
15	-	V. Hudson (H1) Eruption*	PC-18	-	240	170	Mean Pooled Age	6850	160	7660	240	300

*from Stern (2008)

Table 1 - online version

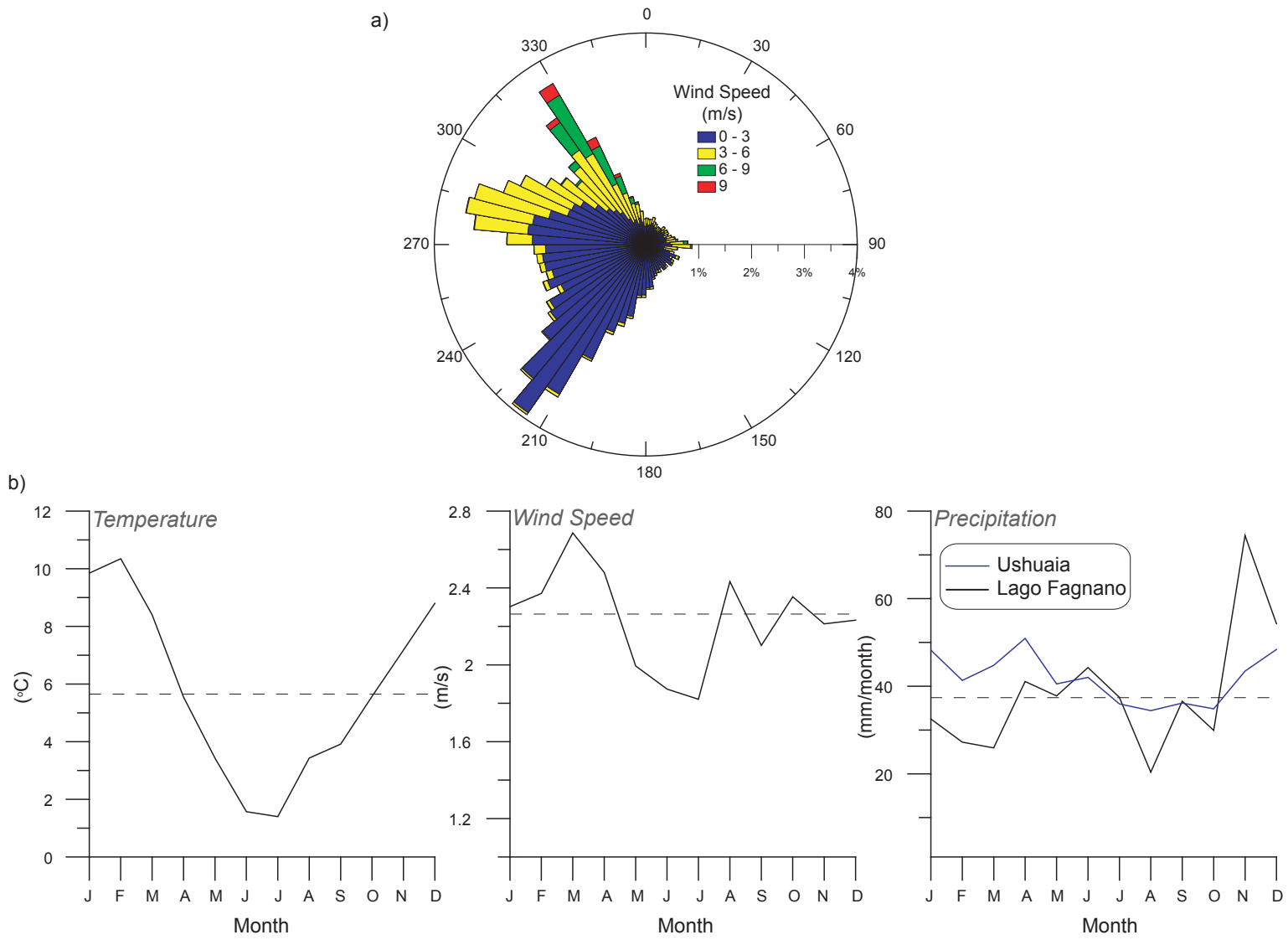

Supplemental Figure 1

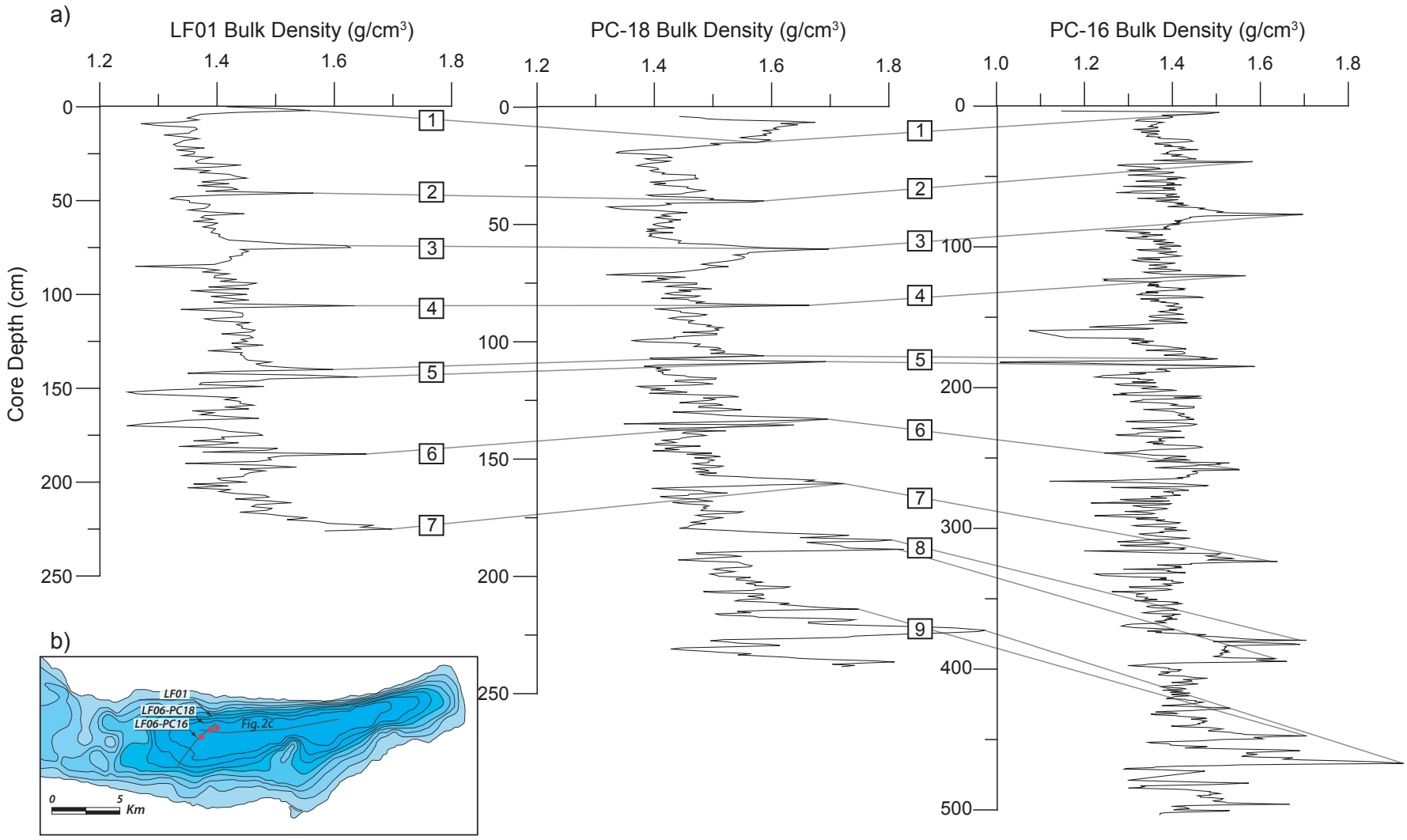

Supplemental Figure 2